Arabian Journal of Geosciences (2021) 14:2644
https://doi.org/10.1007/s12517-021-09035-6

ORIGINAL PAPER

Early Miocene (Aquitanian–Burdigalian) *Clypeaster* and *Schizaster* fauna (Echinoidea: Clypeasteroida, Spatangoida) from Fırat Formation, Diyarbakır, Southeastern Anatolia

İhsan Ekin[1]

Received: 12 October 2021 / Accepted: 18 November 2021

Abstract
Species belonging to Clypeasteroida and Spatangoida orders are common and abundant in carbonate deposits of the Miocene sedimentary sequences of the Mediterranean region. The current paper deals with the notifying of the *Clypeaster* and *Schizaster* fauna (Echinoidea: Clypeasteroida, Spatangoida) from early Miocene (Aquitanian–Burdigalian) of the Fırat Formation in Diyarbakır (Eğil town), Southeastern Anatolia (Turkey), and their palaeoenvironmental conditions. Eleven specimens have been detected as follows: *Clypeaster latirostris* (Michelin, 1861) (specimen CLL-1, CLL-2), *Clypeaster michelotti* (Agassiz, 1840) (specimen CLM), *Clypeaster altus* (Klein, 1734) (specimen CLA) and *Clypeaster intermedius* (Des Moulins, 1837) (specimen CLI-1, CLI-2) from Clypeasteroida order, and *Schizaster eurynotus* (Sismonda, 1841) (specimen SCE-1, SCE-2), *Schizaster parkinsoni* (Defrance, 1827), (specimen SCP-1, SCP-2) and *Schizaster lovisatoi* (Cotteau, 1895) (specimen SCL) from Spatangoida order. Southeastern Anatolia consists of soil and rock units (approximately 120,000 km^2) from the Cambrian to the Miocene. The Miocene sequences of Southeastern Anatolia extend to Çermik, Ergani, Dicle, Eğil and Hani districts (Diyarbakır) in the north, and Harran (Urfa) and the Syrian border in the south. The article creates an annotated species list with notes on specific aspects of palaeogeographic distribution of Echinoids (Clypeasteroida, Spatangoida) from the early Miocene of Fırat Formation in Southeastern Anatolia. Furthermore, since the fossil species identified prefer neritic and sandy-clay habitats, they indicate the tropical climate of the region and become useful for paleoenvironmental reconstructions. Lastly, these data will contribute to providing data for new paleoenvironmental studies by palaeontologists and geologists, and be a pioneer for new fossil records and paleological studies.

Keywords *Clypeaster* · *Schizaster* · Early Miocene · Fırat Formation · Southeastern Anatolia

Introduction

As the Earth passed from the Oligocene to the Miocene and Pliocene, the climate gradually cooled down and formed a series of ice ages. Between 17 and 15 Ma, Miocene climate optimum was followed by an intervening period of global climate variability between 15 and 14 Ma, as a result of carbon cycle variability, expansion of Eastern Antarctic ice sheet, and atmospheric and oceanic cooling (Woodruff and Savin 1991; Flower and Kennett 1994; Zachos et al. 2001; Greenop et al. 2014). The climatic and tectonic changes led up to suitable conditions for the proliferation of marine fossils in the Anatolian layer and made this peninsula fossil-rich treasure, like an open geology laboratory with its fossils left by the Tethys Ocean that has reigned for millions of years, with all kinds of rocks and schist representing all geological epochs (İnan 2008).

Echinoderms speedily diversified and reached a worldwide distribution in the Eocene and Miocene Epochs and constitute a resistant and morphologically six major groups that comprise Echinoidea (Sea urchins and Sand dollars), Asteroidea (Starfish), Crinoidea (Sea lilies and Feather stars), Ophiuroidea (Brittle stars and Basket stars), Holothuroidea (Sea cucumbers) and Concentricycloidea (Sea daisies) (Ghiold and Hoffmann 1986; Mooi 1989; Smith 2001; Nebelsick and Kroh 2002; Alvarado and Cortés 2009). Environmental conditions, habitat, skeletal structure, periods

Responsible Editor: Attila Ciner

✉ İhsan Ekin
ekinihsan@gmail.com

[1] Energy Systems Engineering, Faculty of Engineering, Şırnak University, Şırnak, Turkey

Published online: 25 November 2021

and epochs are significant factors on the preservation and fossilization potential of echinoderms (Greenstein 1995; Dickson 2004). Undoubtedly, they are considered exceptional research materials for palaeoenvironmental reconstructions, due to their high preservation potential as full tests, fragments or skeletons. Their fossils can be found in various sedimentary environments that permit reconstructions along the facies boundaries, and to revive their past, it is possible to apply functional morphology to their skeletons that are highly adapted to the habitats as well as their resistant calcareous skeletons make them possible to encounter them in the environment (Mancosu and Nebelsick 2016).

Clypeasteroida order includes a large number of extant and living species. They can live in many different biogeographical environments, specifically shallow water environments, and represent significant members of the benthic invertebrate communities. In the middle Eocene, they quickly diversified, reaching a worldwide distribution, and today they are one of the highly successful and morphologically diverse groups (Mooi 1989; Nebelsick and Kroh 2002; Mancosu and Nebelsick 2017a). Furthermore, clypeasteroids possess tough test, a high degree of interlocking reinforced by calcareous struts penetrating adjacent coronal plates, and have higher preservation potential than other irregular forms like thin-plated spatangoids (Nebelsick and Kroh 2002; Belaústegui et al. 2012; Mancosu and Nebelsick 2013). *Clypeaster* genus of Clypeasteroida comprises nearly 50 extant and approximately 350 extinct samples (Kroh and Smith 2010; Mihaljević et al. 2011; Mihaljević and Rosenblatt 2018). On the other hand, Spatangoida (spatangoids) is another echinoid order and constitutes the most diverse Sea urchin groups, with about 250 extant species, and with a fossil record dating back to the Jurassic, including more than 80 extinct genera. The order commonly includes the families Spatangidae, Schizasteridae, Loveniidae and Brissidae. Particularly, schizasterids is one of the popular groups of Spatangoida and has ovate or heart-shaped tests with deep anterior sulcus, slightly pointed to the rear (Serafy and Fell 1985; Walker and Gagnon 2014; Ziegler et al. 2020). Generally, the test of spatangoids consists of a radiating series of columns of adjoined plates (Mooi 2020).

Clypeasteroids, spatangoids, gastropods and bivalves are among the major groups of the marine invertebrate assemblages of the early Miocene deposits in the province of Diyarbakır, Southeastern Anatolia. In the current paper, it is presented fossil records of early Miocene clypeasteroids and spatangoids species identified in the Eğil town of Diyarbakır. The main objective of the study is to provide information about *Clypeaster* and *Schizaster* fauna (Echinoidea: Clypeasteroida, Spatangoida) from Fırat Formation (Early Miocene: Aquitanian–Burdigalian) and to shed light on the palaeoenvironmental conditions of the region. In addition, the study is to prove that *Clypeaster latirostris* (Michelin, 1861), *C. michelotti* (Agassiz, 1840), *C. altus (Klein, 1734)*, *C. intermedius* (Des Moulins, 1837), *Schizaster eurynotus* (Sismonda, 1841), *S. parkinsoni* (Defrance, 1827) and *S. lovisatoi* (Cotteau 1895) species, which are not identified in the region previously, lived in Eğil (Diyarbakır-Turkey) province during the early Miocene of the Fırat Formation. The first identification of these species in the region will make a significant contribution to future palaeontological, biological, biogeographical and paleoenvironmental studies. It will also be useful on a large scale to correlate these species with the units of the same age.

Geological setting and stratigraphy (Fırat Formation)

The southeast Anatolian region is located in the border region between the Anatolian microplate and the Arabian and Eurasian plates. Cretaceous and younger deposits crop out on the surface of most of Southeastern Anatolia. The lower parts of the sequence are exposed to several anticlines (Fig. 1). Among these are the Amanos Mountains in the west of Gaziantep, the Derik anticline in the south, the Hazro anticline in the north of Diyarbakır and the Zap anticline of the South Hakkari (Şengör and Yılmaz 1981). In Southeastern Anatolia, the geomorphic evolution of the upper basin of the Tigris River reflects the interaction of surface processes and lithospheric deformation and the development of topographic relief since the closing of the Southern Neotethyan Ocean. At the junction of the Arabian Plate, the Tigris River may be viewed as a preceding river system that flourishing since the Miocene (Fig. 1) (Kathleen 2010). Throughout the Quaternary, the Tigris River continued to flow in a wide valley, concentrating the thick alluvium accumulation and forming a series of terraces over time between the south of Batman and Eğil (study area) during Miocene (Keskin 2003). Miocene is an epoch in which tectonic events were very effective in Southeastern Anatolia. The units belonging to Midyat (Mardin) group have completed their deposition regressively, then in the early Miocene, north of the Southeastern Anatolia began to decrease and the sea level started to rise. The Lice Formation (middle Miocene-Langhian and Serravallian) precipitated and the early Miocene (Aquitanian and Burdigalian) (Fırat Formation) bowl closed with the compression tectonics (Yılmaz 1993; Hüsing et al. 2009).

The oldest unit in the Diyarbakır area consists of overlap and an allochthonous mass that moves from the north to the south Miocene units (Fig. 1). Different phases from Upper Cretaceous to Miocene are known, and a belt with many thrusts is formed along the line (Fig. 1). This belt, which is shown as a geological line, can be observed along the Çermik-Ergani-Dicle-Lice-Kulp line (Genç, 1985). The two most significant members of this allochthonous mass

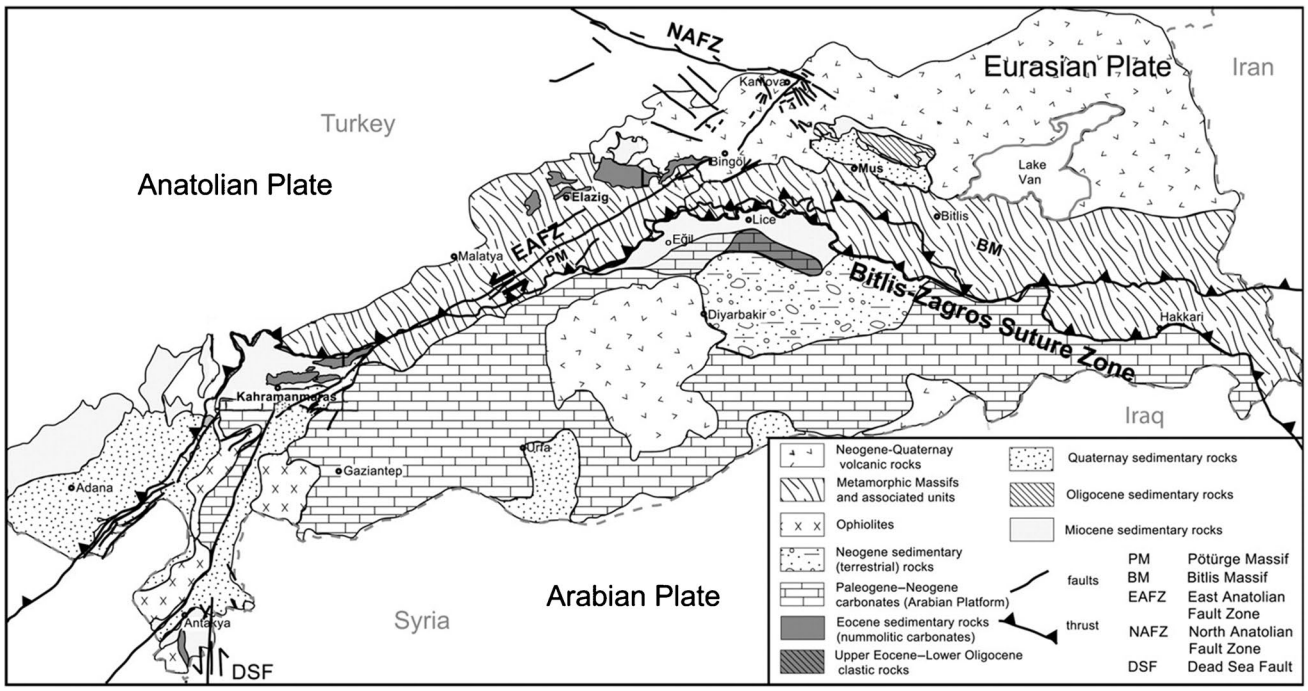

Fig. 1 Geological map of Southeastern Anatolia with major tectonic structures and distribution of early Miocene sedimentary rocks in Diyarbakır which covers the studied area, Eğil (modified from Şenel 2002 and Hüsing et al. 2009)

are ophiolites and metamorphic rocks which are dominantly made of marble. On the other hand, Cretaceous rocks are generally represented by thin-bedded pelagic limestones. In the Eocene, the region turned into a wide carbonate platform and thick limestone levels precipitated (Fig. 1). While shallow shelf carbonates and reefal limestones were deposited in the eastern part of the region, a sequence of clay-marl, chalky clayey limestone intercalations containing deep limestone levels in the western part of the region was deposited during Miocene (Fig. 1). In general, 3 different formations can be distinguished around Dicle, the town of Diyarbakır considered the centre of the Miocene region. At the bottom (in the south), there is the Early Miocene-aged Fırat Formation belonging to the Silvan Group, on the upper side (in the north) the Middle Miocene-aged Lice Formation belonging to the Silvan Group, and above (upper north) the Lice Formation belonging to the Late Miocene-Early, Middle-Upper Miocene-aged Şelmo Formation (Fig. 2) (Yılmaz and Duran 1997; Hüsing et al. 2009; Yeşilova et al. 2018).

The Fırat Formation (Aquitanian and Burdigalian) is located and outcrops in Dicle, Eğil, Hani, Çüngüş, Hazro and Çermik districts in Diyarbakır, along the right bank of Tigris river, in the valley of Zori Stream in Ergani district, Sason district in Batman province, Cizre (Şırnak), Pervari (Siirt), Şemdinli (Hakkari), Kasrık strait north of Cizre district (Yılmaz and Duran 1997). This Formation consists of cream, beige, white, pinkish grey coloured, brittle, sometimes thin, sometimes very thick rocks as well as red algae, bryozoa, coral, large benthic and echinoid fossils and their fragments and mollusc (mostly gastropods and bivalves) shells, reef/bench type limestones (Fig. 3). The outcrops of the Dicle-Lice-Hazro-Eğil belt begin with a ground conglomerate containing variegated, poorly sorted limestone and blocks. The age of the Formation has been determined as Aquitanian–Burdigalian and its environment has been determined as shelf edge-bank/reef (Yılmaz and Duran 1997). The Fırat Formation is distinguished from the limestones belonging to the surrounding Formations by its lighter colour, brittleness, a significant amount of macrofossils and an excess of marl content. The name of the Formation is coming from the carbonates on the edge of the Fırat River near Birecik District. The Formation is divided into four facies (Fig. 2): (A) Grey-beige coloured conglomerate facies: the pebbles and stones that form the facies consist of schist, marble, quartz, serpentinite, radiolarite and limestone structures. The conglomerate should be carbonating cemented, yellow-pink coloured, poorly sized and poorly rounded and beige-yellow coloured, partly deformed. (B) Limestone facies: this facies includes beige-yellow coloured, degraded, deformed and chalked limestones. It cannot be observed in many parts of the land. As the medium, it refers to the marine environment that is calm and calm after the transgression. (C) Yellow-coloured limestone facies: these facies represent yellow-coloured, hard and durable limestones and accompanying clayey intermediate levels. Clayey intermediate

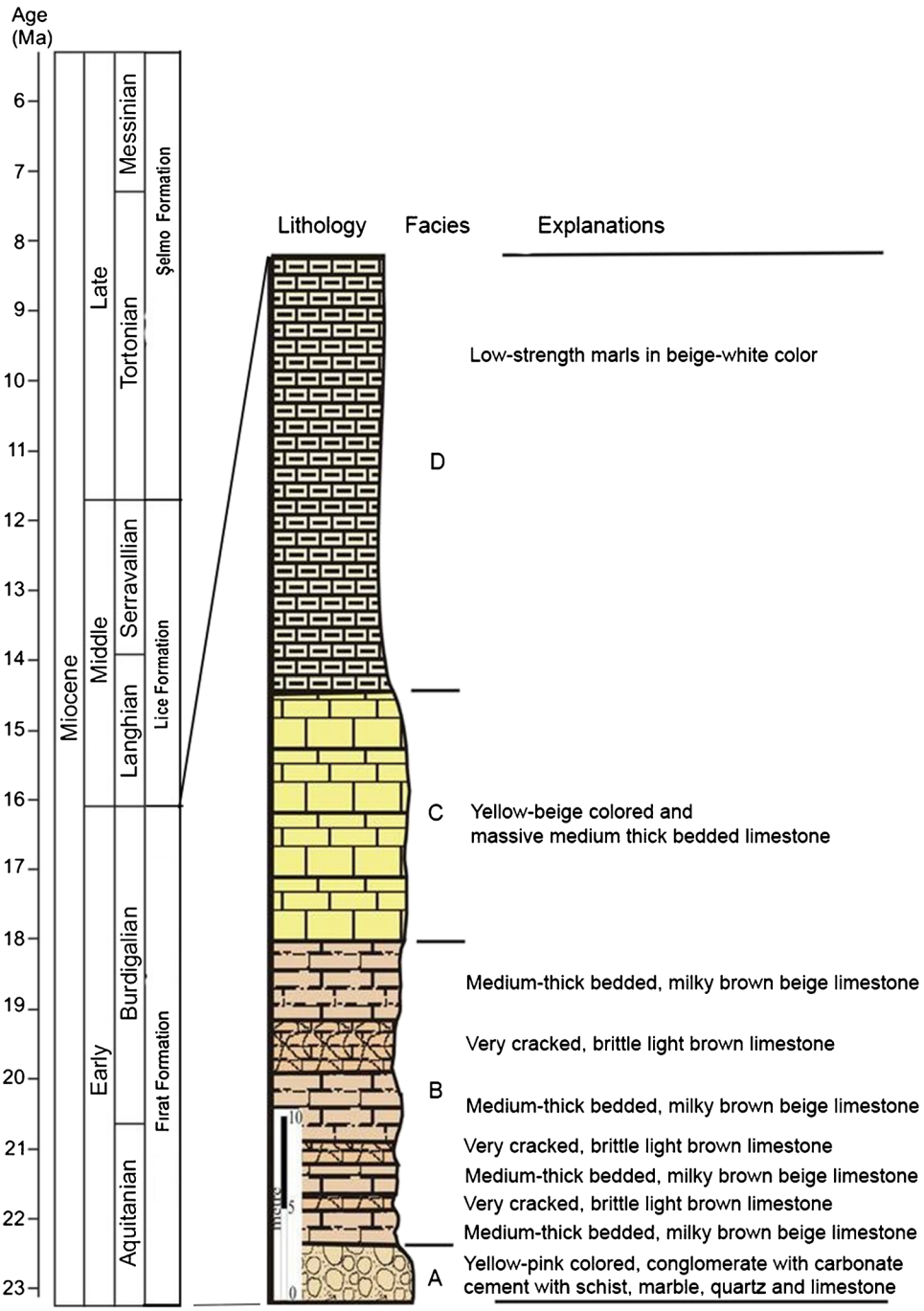

Fig. 2 Cross-section of Fırat Formation (approximately 130 m thick). The specimens *Clypeaster* and *Schizaster* fossils are collected from D and C facies (modified from Yeşilova and Helvacı 2012a)

levels indicate that the water level is low. (D) Beige-white coloured marl facies: This facies is the thickest and the largest one in the Fırat Formation. This facies consists of beige-white coloured marls and clays. The facies represent a sea that becomes shallower. The fact that no sedimentary structure can be observed and it contains abundant carbonate mud shows that this facies is formed under stagnant shallow water conditions away from wave activity (Duke et al. 1991; Yeşilova and Helvacı 2012a, 2012b; Güngör Yeşilova and Helvacı 2013, 2017; Yeşilova et al. 2018).

Until now, the following taxa have been identified from the Fırat Formation (Yılmaz and Duran 1997), *Homotramatidae*, *Echinoidea*, *Acervulinidae*, *Ostracoda*, *Bryozoa*, *Pelecypoda*, *Bivalvia*, *Cnidaria*, *Gastropoda*, *Miliolidae*, *Rotaliidae*, *Textulariidae*, *Alveolinidae*, *Peneroplidae*, *Heterostegina* sp., *Neoalvepolina* sp., *Miyogypsina* sp., *Globigor spina*, *Miogypsinoides* sp., *Austrotrillina* sp., *Sphaerogypsina* sp., *Archaias* sp., *Peneroplis* sp., *Borelis* sp., *Elphidium* sp., *Rotalia* sp., *Cycloclypeus* sp., *Amphistegina* sp., *Lepidocyclina* sp. and *Nephrolepidina* sp.

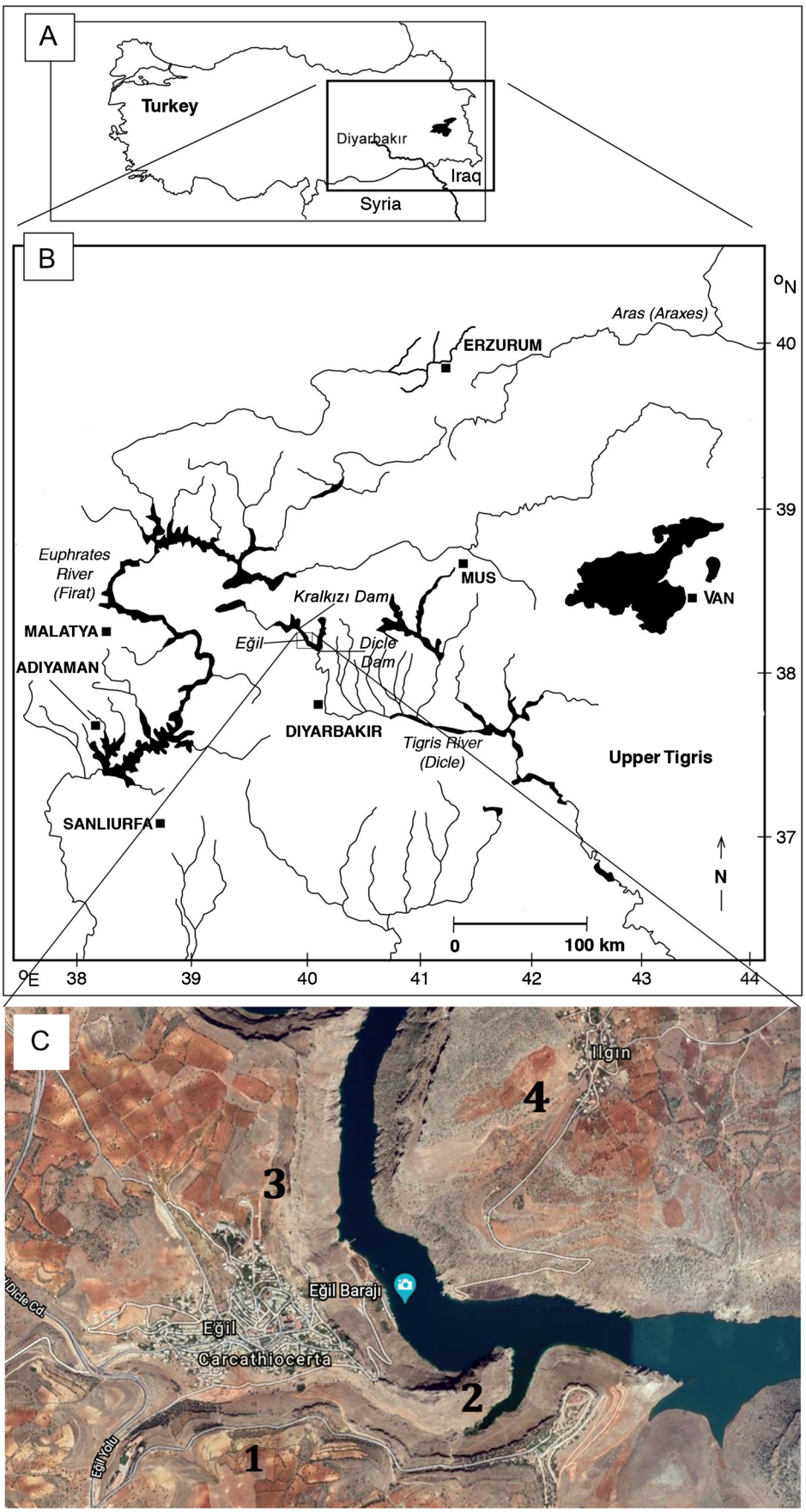

Fig. 3 **A** Map of Turkey. (**B**) Southeastern Anatolia and Primary rivers: the Aras (Araxes), the Fırat River, the Tigris River and big dams of Southeastern Turkey. (**C**) The banks of the Tigris River, Dicle Dam and the locations (1, 2, 3, 4) of the samples

Material and methods

This study is based on *Clypeaster* and *Schizaster* fauna (Echinoidea: Clypeasteroida, Spatangoida) collected from Southeastern Anatolia, Diyarbakır (Eğil town) (Altitude: 866 m, Coordinate: 38° 15′ 0.11″ N / 40° 08′ 0.59″ E) (Fig. 3), throughout the succession between 2015 and 2020, in the Fırat Formation. Eğil town is located approximately 48 km north of Diyarbakir and between the Kralkızı and Dicle Dams. Fossil records of the species have been collected around Eğil town, just above (between 0 and 1 m) sandy-clay area. The collection area was eroded due to the Tigris River bed, which made the samples closer to the surface. The collection areas are labelled as locations 1, 2, 3 and 4 and the codes of samples expressed in the parenthesis are given in line with the names of the species (first 2 letters of the genus name and the first letter of epithet name); thus, expressing different samples for same species is facilitated and confusion is eliminated.

Four locations of 11 fossil records are as follows (Fig. 3C): Location 1 (1 km south of Eğil town) (1 sample): *Clypeaster latirostris* (Michelin, 1861) (specimen CLL-1). Location 2 (Eğil Castle area) (2 samples): *Clypeaster michelotti* (Agassiz, 1840) (specimen CLM), *Schizaster lovisatoi* (Cotteau 1895) (specimen SCL). Location 3 (1 km north of Eğil town) (3 samples): *Clypeaster altus* (Klein, 1734) (specimen CLA), *Clypeaster intermedius* (Des Moulins, 1837) (specimen CLI-1, CLI-2). Location 4 (west of Ilgın village, 2 km east of Eğil town) (5 samples): *Schizaster eurynotus* (Sismonda, 1841) (specimen SCE-1, SCE-2), *Schizaster parkinsoni* (Defrance, 1827), (specimen SCP-1, SCP-2), *Clypeaster latirostris* (Michelin, 1861) (specimen CLL-2).

The soft soil fragments on the fossil specimens were cleaned with a fine brush and preparation needle; if necessary they were cleaned by water and NaOH solution and then labelled and stored in Engineering and Biology Laboratory of Şırnak University. The help of the experts was obtained for taxonomy and identification of the samples on species and genus levels. Species and genera identifications were made based on echinoids morphology as well as collected specimens compared to those in invertebrate fossil-library databases. To identify the species, the contributions and diagnoses of expert palaeontologists were used. The dimensions of the samples were measured by using a precision ruler and digital calliper. High-resolution photographs of the samples were photographed in the Şırnak University, Engineering and Biology Laboratory by using Nikon Coolpix P900 camera and 83xZoom-NIKKOR ED Glass Lens. Measurements were made of test length (L), maximum test width (W) and maximum test height (H) (from apical points). All dimensions of the samples are expressed in millimetres and shown by the scale bar on the photographs. Some of the other measurements such as the location of the apical centre, width of ambulacra, width and length of anterior ambulacra (III), length and width of anterior and posterior petaloid pairs, location of the peristome and periproct are expressed on the samples by placing a white measure scale on the photographs.

Systematic palaeontology

Class: Echinoidea (Leske, 1778).
Superorder: Gnathostomata (Zittel, 1879).
Order: Clypeasteroida (Agassiz, 1872).
Family: Clypeasteridae (Agassiz, 1835).
Genus: *Clypeaster* (Lamarck, 1801).

Clypeaster latirostris Michelin, 1861 (Figs. 4 and 5)

1864 *Clypeaster latirostris*, Wright, p. 479.
2010 *Clypeaster latirostris*, Pereira, p. 206.
2016 *Clypeaster latirostris*, Mancosu and Nebelsick, p. 147, fig. 6C.

Diagnostic features and remarks

The test is pentagonal, but it has a slight extension towards the front. The front of the test is wide and triangular. The oral surface is flat and slightly sunken towards the centre. Food groves are prominent and star-shaped, and slight submergence towards the peristoma. The apical surface is of medium swelling. Petals rise vertically and converge around the apical disc. Petals are long, protruding and open at the ends. The apical disc has five gonopore. Interambulacral regions are flat at the beginning and slightly curved downwards. The peristome is sunken and in the centre of the oral surface. The pericropt is located behind the rear tube foot. *C. latirostris*, co-occurring species with *C. intermedius*, is distinguished from *C. intermedius* by its lower test height, with the less raised ambulacral area, subequal test length and width, thinner margin, more flattened ventral surface and more broad, and a very shallow infundibulum.

***Clypeaster latirostris* Michelin, 1861, (Specimen CLL-1)** Figure 4 L: 91 mm (as eroded), W: 82 mm (as eroded), H: 30 mm (as eroded)

Description: The test is moderately large, pentagonal and the length and width of the test are subequal. The test margins are normally thin; however in specimen CLL-1, the edges are not well protected, eroded, and this caused the sample to be measured slightly smaller than its normal size. The maximum length lies from anterior ambulacrum III to interambulacrum 5 (Fig. 4A). The maximum width lies from ambulacrum II and IV. The test is low with a moderately upraised petaloid area. Petals are moderately long, rather wide, flattened in the inter-pores, but protruding, open at the distal ends of the petals (Fig. 4E). All ambulacra are petaloid, straight and approaching each other distally, not closed. The apical disc is not fully visible due to

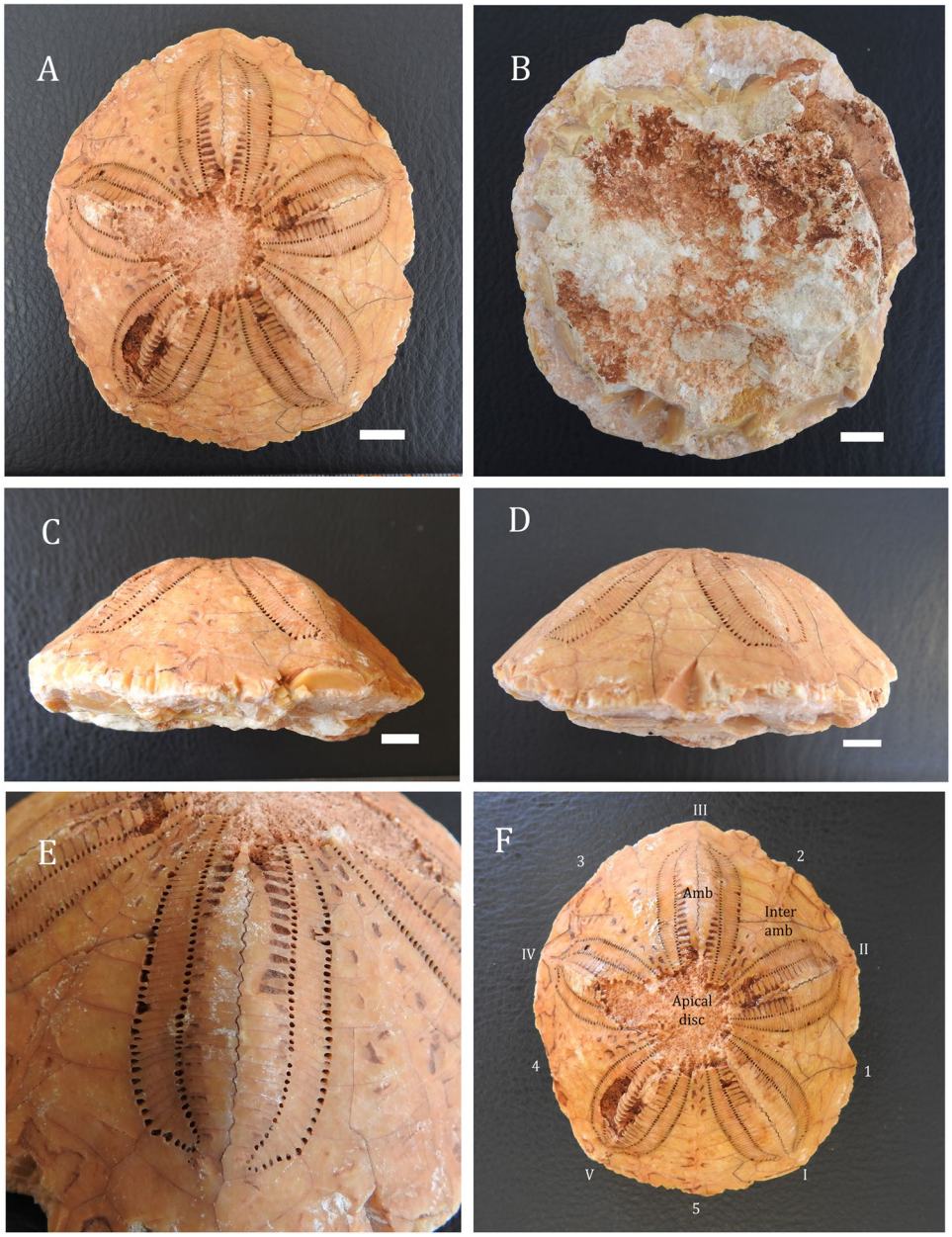

Fig. 4 *Clypeaster latirostris* (Michelin, 1861) (specimen CLL-1). **A** Apical (aboral) view, **B** (oral) ventral view, **C** posterior view, **D** lateral view and **E** close-up of ambulacrum III (petaloid III). Petals (ambulacra) have two rows of respiratory podia. **F** It is seen bilaterally symmetrical test composed of 10 double columns of plates, 5 interambulacra (labelled 1–5) and 5 ambulacra (labelled I–V). The anterior part is ambulacrum III; the posterior part is interambulacrum 5. amb, ambulacrum; inter amb, interambulacrum. Each white scale bar equals 10 mm

destruction. The food grooves on the oral surface cannot be fully observed at the bottom due to rock fragments. The frontal petaloid (III) is the longest; the paired petals (I–V and II–IV) are subequal in length, the anterior ones being a little bit shorter than the posterior ones in the specimen CLL-1 (Fig. 4A). The interambulacra are moderately inflated (Fig. 4C, D).

***Clypeaster latirostris* Michelin, 1861, (specimen CLL-2)** Figure 5 L: 90 mm (as broken), W: 103 (as broken) mm, H: 31 mm

Description: Due to broken edges of the test, the pentagonal shape is not well visible, but normally the test of the species is pentagonal. The aboral (apical) surface is slightly raised, like in CLL-1. Margins are thin (Fig. 5C). In specimen CLL-2, some part of the edges is well preserved, but some of them were broken (Fig. 5A). The oral (ventral) surface is flat, the flatness of the oral surface is an important feature of *C. latirostris,* and the peristome is invisible due to the rock fragment attached to the bottom. However, food grooves can be distinguished. All five petals are markedly petaloid, moderately long, rather wide, flattened in the inter-pores and distally inclined closed, but open in the endpoint (Fig. 5E) as in CLL-1 (Fig. 4E). The anterior petaloid (Ambulacrum III) is the longest one. Other paired

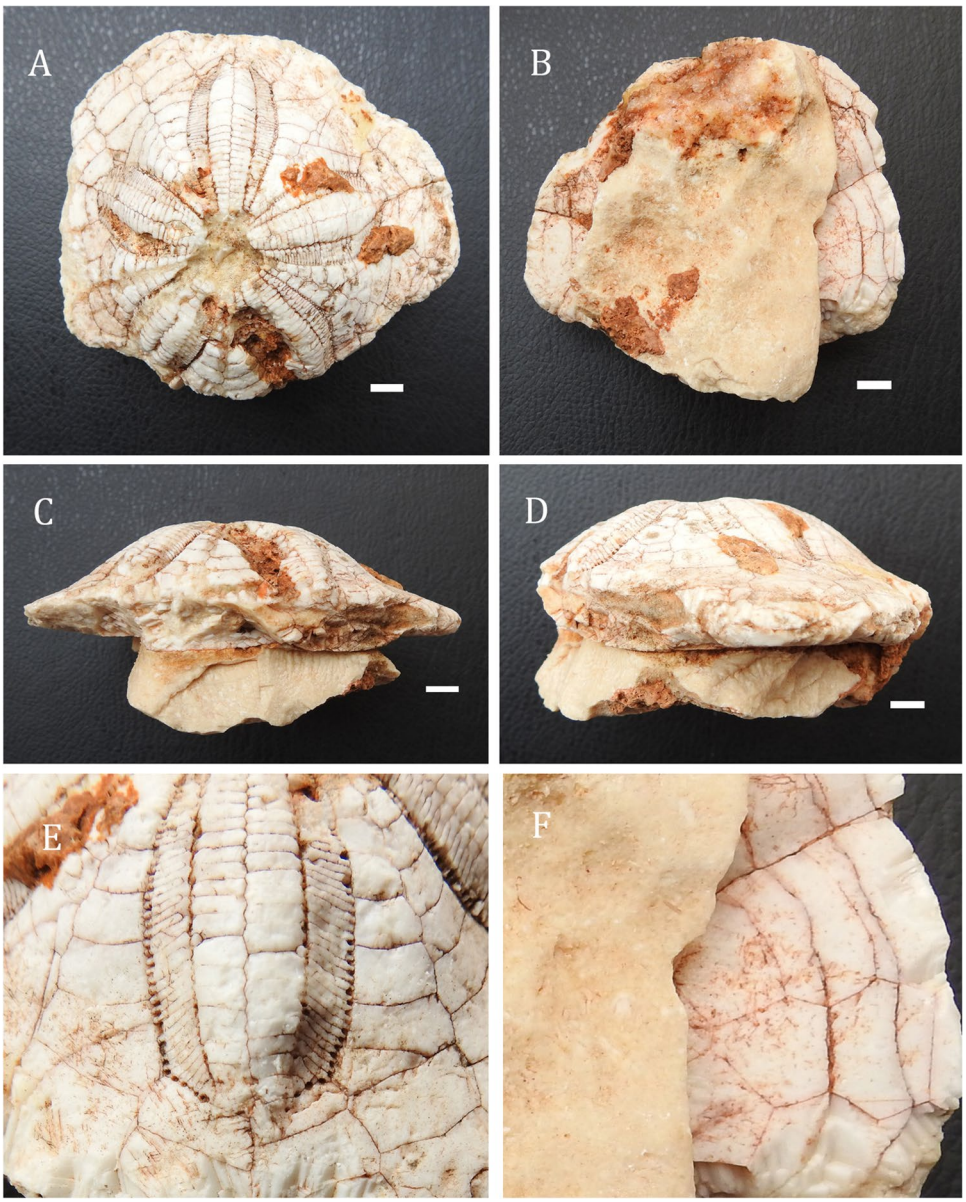

Fig. 5 *Clypeaster latirostris* (Michelin, 1861) (specimen CLL-2). **A** Apical (aboral) view, **B** ventral (oral) view with rock fragment, **C** posterior view, **D** lateral view and **E** close-up of ambulacrum III (petaloid III). **F** Close-up of the flat ventral surface. Each white scale bar equals 10 mm

petals are subequal (Fig. 5A). The pair of pores in all petals can be seen clearly. The porous areas are lightly pressed and relatively wide. Interambulacra is moderately inflated and noticeable with details. The apical part is damaged, so gonopores cannot be observed.

Clypeaster michelotti Agassiz, 1840 (Fig. 6)

1877 *Clypeaster michelotti*, Dames, p. 25.
1906 *Clypeaster michelotti*, Lambert, pl. XX, p. 12.
1961 *Clypeaster michelotti*, Ferreira, and da Veiga, p. 542, fig. 35.
1972 *Clypeaster michelotti*, Marcopoulos-Diacantoni, p.145, pl. II, fig. 1

Diagnostic features and remarks

The test is pentagonal and very smooth. The edges of the test are thinned and the angles are rounded. The apical surface is swollen upward in the ambulacral part. The oral surface is flat and has five food grooves extending into the peristome, which is quite deep. It has thin elongated petaloid ambulacral regions and the petals are open towards the ends. The peristome is small, slightly pentagonal and shallow. Pericropt is submarginal. It differs from other species in rounded edge and pentagonal shape.

The apical surface in the ambulacral part of the *C. michelotti* is swollen than the *C. latirostris* species. *C. michelotti* has thin elongated petaloid ambulacral regions, but in *C. latirostris* the petaloids are wider. On the other hand, C. *intermedius* has a larger test structure and a higher apical region compared to *C. michelotti* and *C. latirostris*.

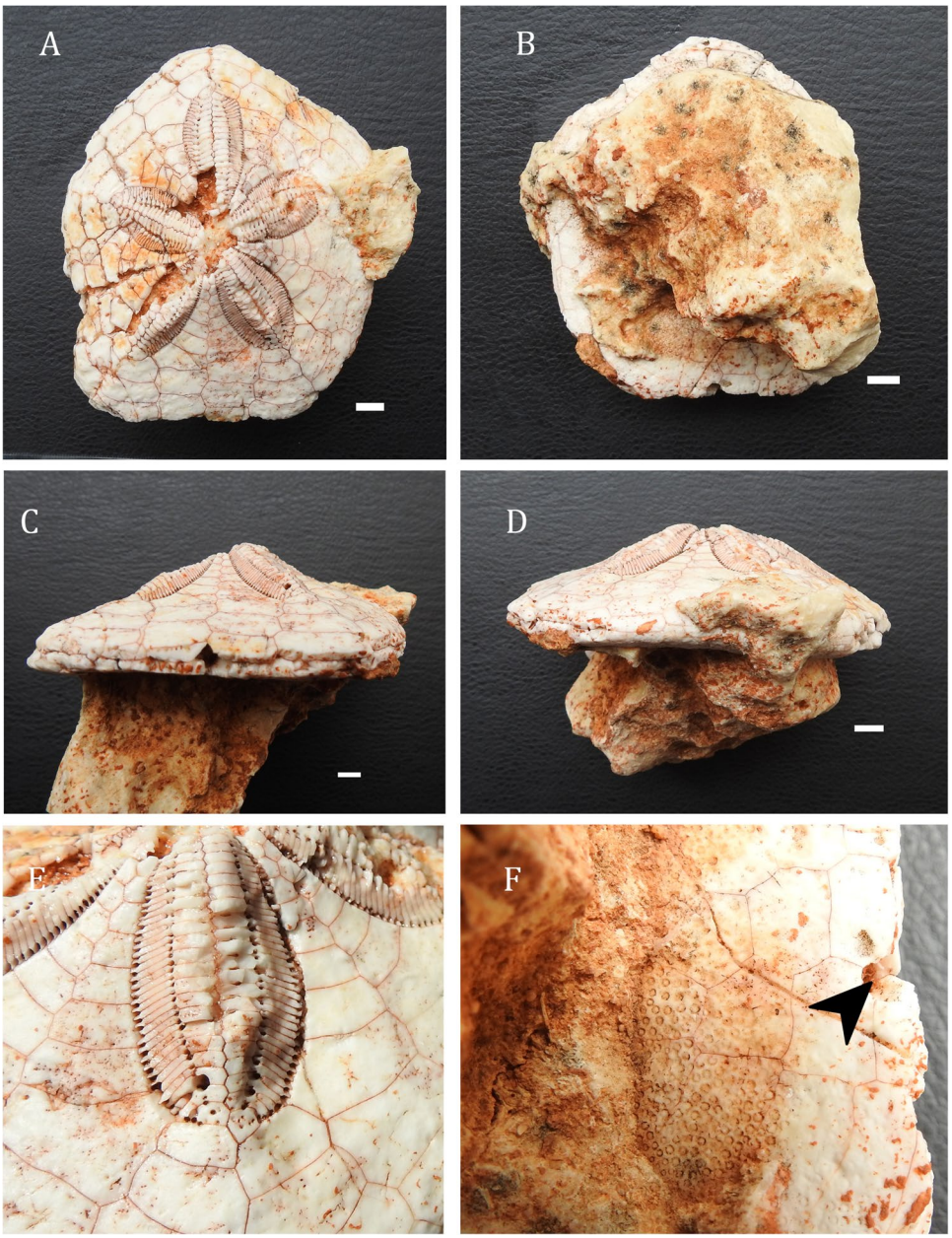

Fig. 6 *Clypeaster michelotti* (Agassiz, 1840) (specimen CLM). **A** Apical (aboral) view, **B** ventral (oral) view with rock fragment, **C** posterior view, **D** lateral view and **E** close-up of ambulacrum I (petaloid I). **F** Close-up of the ventral surface and pericropt (black arrow) and numerous spine tubercles. Each white scale bar equals 10 mm

***Clypeaster michelotti* Agassiz, 1840, (specimen CLM)** Figure 6 L: 102 mm, W: 94 mm, H: 31 mm

Description: The test is pentagonal and slightly anteroposteriorly elongated. The margins of the test are thin and well preserved (Fig. 6C, D). The apical system is flattened but deformed in some places. The ambulacra are petaloid in shape and incline inwards. The anterior petaloid (Ambulacrum III) is the longest (Fig. 6A). The pair of pores in the petals stand closer together, on the contrary of CLL-1 and CLL-2 specimens, and open in the distal part at close range (Fig. 6E). The ambulacra plates are smoothly rectified with submerged interambulacra plates. The length of the central porofore zone and the pair of rear porofore zone are slightly longer than the lateral pair length. The ventral surface is flat (Fig. 6B), the peristoma and food grooves are not visible due to the rock fragment attached to the basement, but the periproct is visible at the ventral surface (Fig. 6F). Since the apical system is damaged, gonopores are not visible.

Clypeaster altus Klein, 1734 (Fig. 7)

1958 *Clypeaster altus*, Imbesi, p. 28, fig. 1,1a, 2, 2a, 2b.

1967 *Clypeaster altus*, Marcopoulou-Diacantoni, p. 359, pl. III, fig. 1, la, pl. IV, fig. 2.

1969 *Clypeaster altus*, Mitrovic-Petrovic, p. 126, fig. 2, 2a.
1985 *Clypeaster altus*, Marcopoulou-Diacantoni, p. 103, 105, 108, 159, pl. III.
1998 *Clypeaster altus*, Philippe, p. 122.
2000 *Clypeaster altus*, Marcopoulou-Diacantoni, p. 177.
2007 *Clypeaster altus*, Tsaparas et al., pl. 1A, p. 228.

Diagnostic features and remarks

Clypeaster altus has a high-domed, large, pentagonal and commonly campanulate test. The ambulacral region is swollen and pyramid-like in appearance and it rises and converges around the apical disc. The aboral surface has long five broad petals possessing broad poriferous zones which almost close distally. The oral surface has a large infundibulum and is flat. Ambulacral petals form petaloid open with the elevated intermediate region. The interambulacral regions are in the submerged position from the apical disc to the periphery. The apical disc contains five gonopore. Pericropt is rounded.

***Clypeaster altus Klein*, 1734, (specimen CLA) (Fig. 7)** Figure 7 L: 101 mm (as eroded), W: 92 mm (as broken) H: 43 mm

Description: Its overall appearance is bulging and this is the most important feature distinguished *C. altus* from most other species. It has got a large, high-domed, commonly campanulate test (Fig. 7A). The edges of the test should be slightly longer and have five corners; however, in the specimen CLA, the test margins are not well preserved. The dimensions of the specimen are normally bigger than calculated, because dimensions were measured as

Fig. 7 *Clypeaster altus* (Klein, 1734) (specimen CLA). **A** Apical (aboral) view, **B** ventral (oral) view, **C** posterior view, **D** lateral view and **E**: close-up of ambulacrum III. **F** Ventral side and food grooves. Each white scale bar equals 10 mm

the broken states, as in all the broken samples in the current study. The edges of the test are relatively round and thick. Ambulacra are quite long, protruding and wide open and slanted (Fig. 7E). Ambulacrum II is broken (Fig. 7A). The ventral surface (oral) is nearly flat, slightly collapsed in and in the axis of ambulacra II, III, IV and V simple narrow unbranched food grooves parts are visible (Fig. 7F). Peristome and pericropt are not visible. The specimen has got large infundibulum at the oral surface, one of the other significant features of *C. altus* (Fig. 7F).

Clypeaster intermedius Des Moulins, 1837 (Figs. 8 and 9)

1967 *Clypeaster intermedius*, Marcopoulou-Diacantoni, p. 370, pl. VI.

1985 *Clypeaster intermedius*, Marcopoulou-Diacantoni, p. 128, 134, 159, 176, pl. X-XII.

1998 *Clypeaster intermedius*, Philippe, p. 302, pi.11, fig. 4-6, pi. 12, fig. 1-4.

2000 *Clypeaster intermedius*, Marcopoulou-Diacantoni, p. 178, pl. Ill, fig. la, b, pl. V, fig. 3a, b, pl. VI, fig. 1.

2007 *Clypeaster intermedius*, Tsaparas et al., pl. 2F, G, p. 230.

2017 *Clypeaster intermedius*, Mancosu and Nebelsick, p. 632, fig. 4F.

Diagnostic features and remarks

The test size is large and pentagonal. Marginal timidity is relatively low. The test profile is moderately inflated slightly concave to flat. The aboral surface is slightly cone-shaped. The lower surface is slightly sunken starting from the periphery towards the centre. The petals that form the ambulacral regions, rise slightly and unite around the apical disc. The impaired ambulacral anterior zone is more narrow and elevated. Petals are protruding and their ends are open. The apical disc has five gonopore. Interambulacral regions are slightly sunken from the apical disc towards the periphery. The oral surface has a relatively small infundibulum. The peristome is in the centre of the oral surface and submerged. Pericropt is rounded.

***Clypeaster intermedius* Des Moulins, 1837, (specimen CLI-1) (Fig. 8)** Figure 8 L: 110 mm (as eroded), W: 102 mm, H: 36 mm

Description: The test is large, slightly anteroposteriorly elongated, with a pentagonal shape. The test margin is rounded and the pentagonal outline thick. The lateral margins are reasonably indented in interambulacra. The profile of the test is low arched, with a slightly upraised petaloid region. The apical disc lies subcentrally. The maximum length stands out from anterior ambulacrum III to interambulacrum 5 (Fig. 8A). The maximum width lies from ambulacrum II and IV (Fig. 8A). The maximum height extends sub-centrally around the apical system. The ventral surface is flattened (Fig. 8B, E) with a broad surface but due to the rock fragment, infundibulum and peristome are not visible (Fig. 8B). All five ambulacra are petaloid, straight and slightly closing distally, but open (Fig. 8E). The poriferous zones are moderately wide and slightly depressed (Fig. 8E). The pair of pores is conjugated anisopores. The interporiferous zones are moderately inflated (Fig. 8A, C). On the oral surface in the axis of ambulacra III and IV simple narrow unbranched food grooves parts are visible (Fig. 8B). Apically the interambulacra are slightly depressed between the petals. The periproct is visible on the ventral surface (Fig. 8F).

***Clypeaster intermedius* Des Moulins 1837, (specimen CLI-2) (Fig. 9)** Figure 9 L: 102 mm (as broken), W: 71 mm (as broken), H: 35 mm

Description: The anterior and posterior parts of specimen CLI-2 are not distinguishable, because of fragmentation. Since two petals are broken, it is not clear which petaloid is the longest and Ambulacrum III. Even if the test is broken, it is understood from its petals that it is pentagonal and large. The margin of CLI-2 is round and has medium thickness. The profile has a low arch, slightly raised petaloid area (Fig. 9C). The maximum height is located sub-centrally near the apical system (Fig. 9A). The oral surface is broadly flattened. The apical disc extends sub-centrally and is well preserved in the specimen CLI-2. Gonopores are observed conspicuously (Fig. 9E). The connection point of the petals in the apical can be seen. The possible petaloid III is slightly flat and approaching distally, but in an open position. Porous areas are slightly pressed and medium width (Fig. 9F). Intraporiferous areas are moderately inflated (Fig. 9A, C). Simple narrow unbranched food grooves can be seen very well on the oral surface in the ambulacra axes (Fig. 9B). Peristome and pericropt are not seen.

Superorder: Atelostomata (von Zittel, 1879).

Order: Spatangoida (Claus, 1876).

Suborder: Hemiastrina (Fischer, 1960).

Family: Schizasteridae (Lambert, 1906).

Genus: Schizaster (Agassiz, 1835).

Schizaster eurynotus Sismonda, 1841 (Figs. 10 and 11)

1913 *Schizaster eurynotus*, Cottreau, p. 68, 114, fig. 29, pl. 14, figs. 1-6.

1920 *Schizaster eurynotus*, Fourtau, p. 78.

1967 *Schizaster eurynotus*, Marcopoulos-Diacantoni, p. 387, pl. XX, fig. 2.

2003 *Schizaster eurynotus* -Kroh and Nebelsick, p. 167, fig. 5d.

2007 *Schizaster eurynotus*, Kroh, p. 190, figs. 3/r-s.

2010 *Schizaster eurynotus*, Pereira, p. 207, fig. 1j.

2016 *Schizaster eurynotus*, Mancosu and Nebelsick, p. 149, fig. 8/A.

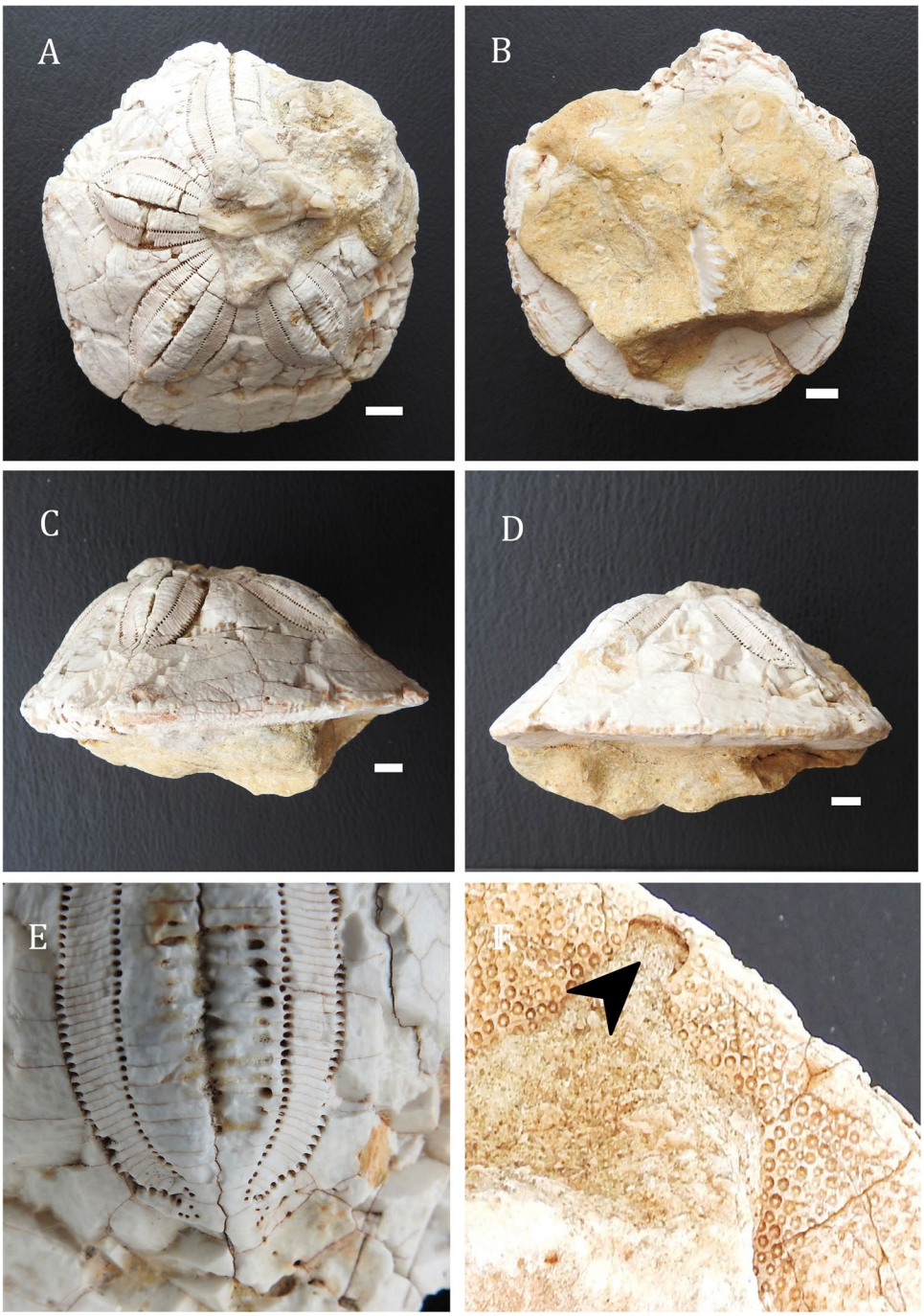

Fig. 8 *Clypeaster intermedius* (Desmoulins, 1837) (specimen CLI-1). **A** Apical (aboral) view, **B** ventral (oral) view, **C** lateral view (right part is posterior, left part is anterior), **D** posterior view and **E** close-up of ambulacrum I. **F** Black arrow show periproct and numerous of spine tubercles on the ventral surface. Each white scale bar equals 10 mm

2017 *Schizaster eurynotus*, Abdelhamied Elattaar, p. 250, pl. 7–1, 1a, 1b, 1c, 2.

Diagnostic features and remarks

Test is ovate with deep anterior sulcus, slightly pointed to rear and carinate. Aboral tuberculation is fine, uniform and dense. The apical disc has two smaller anterior and two large posterior gonopore. The anterior ambulacrum is deeply sunken and becoming less pronounced towards the ambitus. Pore-pairs are in single-column series, specialized for funnel-building tube-feet. Other ambulacra are also deeply sunken, anterior petals much longer and more flexed than posterior petals. It has a small and marginal pericropt, on a near-vertical truncate face. The peristome is weakly labiated, wider than long. Plastron wide and ovate, episternal plates not paired and opposite and not forming a significant part of plastronal area. *S. eurynotus* is distinguished from *S. scillae* (Des Moulins, 1837) by its anteroposterior elongation, shorter posterior petaloid pair and more strongly wedge-shaped profile.

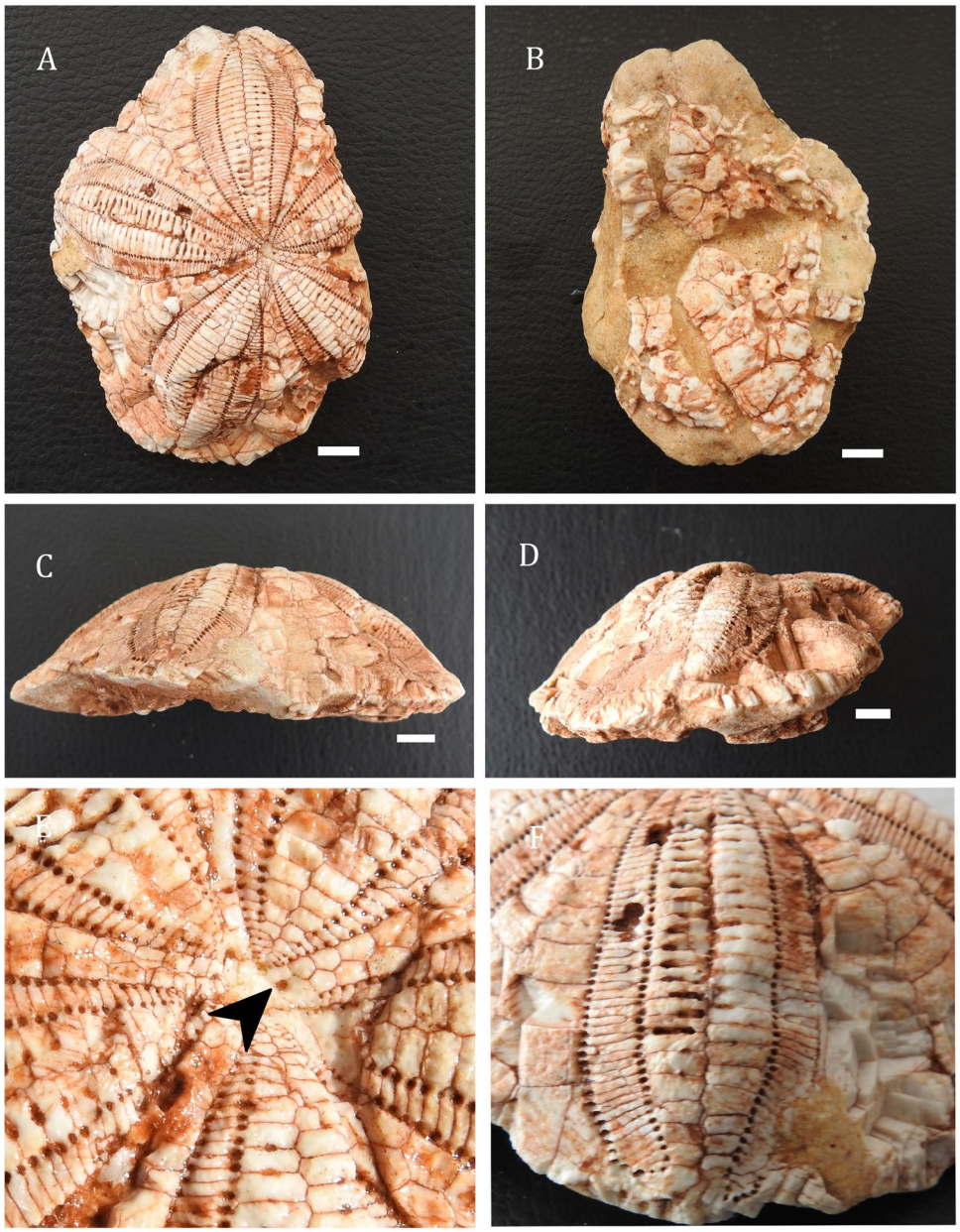

Fig. 9 *Clypeaster intermedius* (Des Moulins 1837) (specimen CLI-2). **A** Apical (aboral) view, **B** ventral (oral) view, **C** possible posterior view, **D** possible lateral view and **E** close-up of the apical disc with gonopores. **F** Estimated potential ambulacrum IV (petaloid IV). Each white scale bar equals 10 mm

***Schizaster eurynotus* Sismonda, 1841, (specimen SCE-1) (Fig. 10)** Figure 10 L: 71 mm, W: 64 mm, H: 29 mm

Description: The outline of the test is heart-shaped and extended anteroposteriorly. It has a wedge-shaped profile. The margin is rounded at the anterior part. In the specimen SCE-1, a slight asymmetry is observed; the right side stands out further anteriorly than the left part (Fig. 10A). The posterior edge is strongly pointed. Periproct and peristome are not visible. The apical centre is situated at the posterior side about 30% of the total length from the posterior point. Ethmolytic four gonopores are present in the centre of the apical disc (Fig. 10F). The anterior petaloid is the longest one. All ambulacra are deeply sunken. Anterior Ambulacrum (III) is more deeply sunken than other petals with its overhanging walls and in a slightly narrower state in the distal region, where the pores are smaller and have less space. The pores are positioned in two straight rows (Fig. 10E). The anterior petaloid pair (II-IV) tips tend to flex slightly laterally. While the posterior double petals are the widest in their mid-points, the frontal petals are the largest near the distal part. The interambulacra are inflated apically, forming high keels (Fig. 10E, A).

***Schizaster eurynotus* Sismonda, 1841 (specimen SCE-2) (Fig. 11)** Figure 11 L: 73 mm, W: 62 mm, H: 31 mm

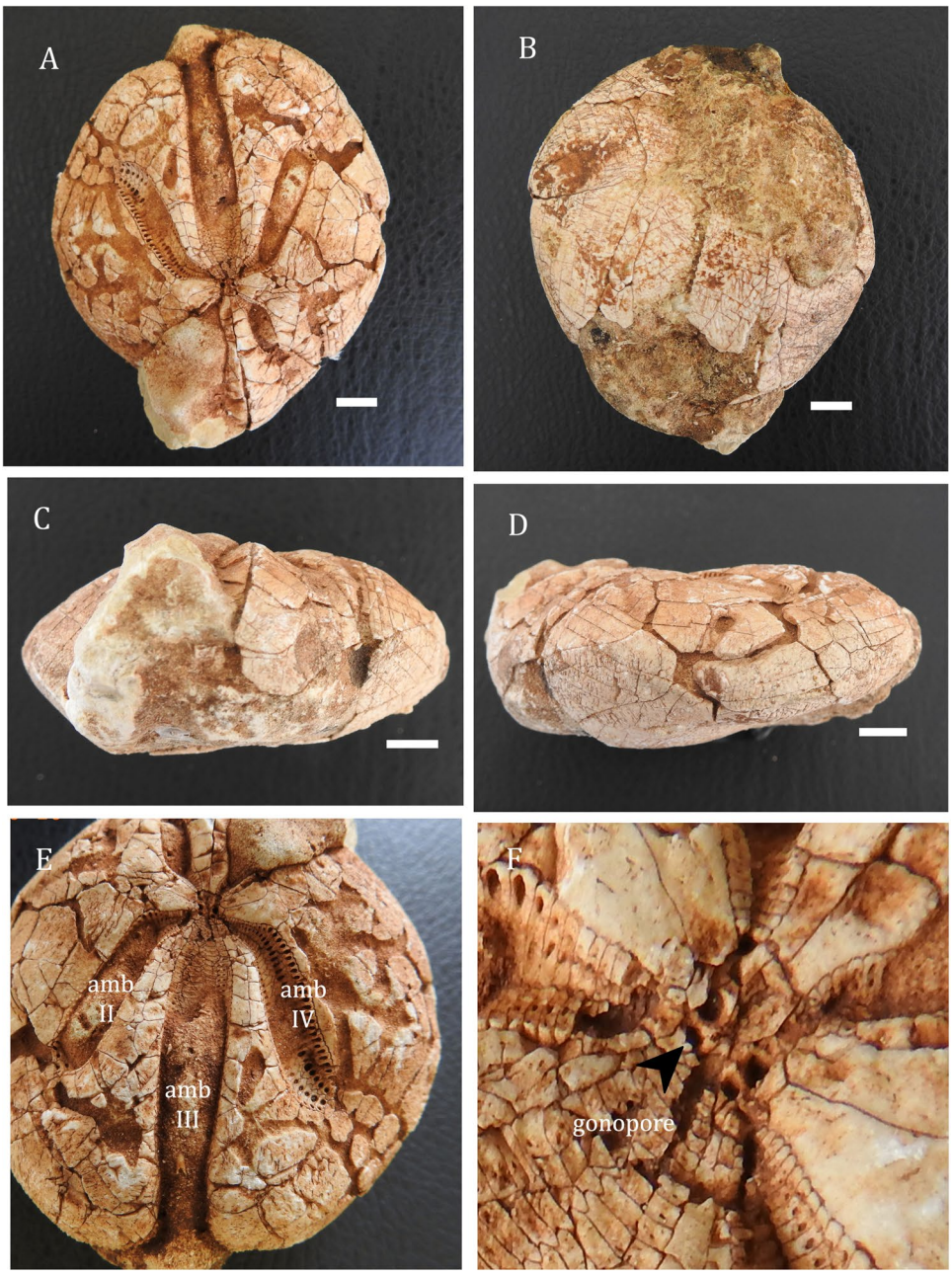

Fig. 10 *Schizaster eurynotus* (Sismonda, 1841) (specimen SCE-1). **A** Apical (aboral) view, **B** ventral (oral) view, **C** posterior view, **D** lateral view and **E** close-up of ambulacrum III, II and IV and apical disc. **F** Four gonopores are seen at the apical disc. Each white scale bar equals 10 mm

Description: The outline of the test is heart-shaped and elongated anteroposteriorly. The test is thick and relatively angular at the back. It has a wedge-shaped profile. The apex is eccentric (backwards). The front ambulacral area is larger than the rear ones. The apical centre stands out posterior of the centre. The ambulacra are all petaloid and deeply sunken. Ambulacrum (III), extends to the apex and is more deeply sunken than others (Fig. 11A). The anterior margin is rounded. On the contrary of specimen SCE-1, in specimen SCE-2, symmetry is observed (Fig. 11A). The posterior margin is sharply pointed (Fig. 11C, D). Traces of ethmolytic (two to four) gonopores are observed (Fig. 11F). Ambulacrum IV is partly broken (Fig. 11A). Pores of ambulacra III are not well observed. The pores in other ambulacra are arranged in two straight rows. The anterior paired petals are longer than the posterior pair. The poriferous zone of the paired petaloid is made up of conjugate elongated isopores (Fig. 11E, F). Periproct and peristomes are not visible.

Schizaster parkinsoni Defrance, 1827 (Figs. 12 and 13)

1908 *Schizaster parkinsoni*, Stefanini, p. 476, tav. XVII, fig. 11, 12.
1933 *Schizaster parkinsoni,* Vautrin, p. 113.

Fig. 11 *Schizaster eurynotus* (Sismonda, 1841) (specimen SCE-2). **A** Apical view, **B** ventral view, **C** posterior view, **D** lateral view and **E** close-up of ambulacrum III, II and IV. **F** Traces of gonopores are seen at the apical disc. Each white scale bar equals 10 mm

1972 *Schizaster parkinsoni*, Marcopoulos-Diacantoni, p. 145, pl. II, fig.1.

2016 *Schizaster parkinsoni*, Mancosu and Nebelsick, p. 146, fig. 5D.

Diagnostic features and remarks

The test has a small size and wedge-shaped profile laterally and heart-shaped from the upper view. The anterior ambulacrum is subequal width and length and shallow. It has non-angular posterior petals. The apex is less eccentric. Anterior ambulacrum is steep. Anterior petals are longer than the posterior petals. Anterior petals are slightly outward towards the ends. Posterior petals are significantly shorter than anterior petals. Apical disc has two gonopores. *S. parkinsoni* is a common early to middle Miocene species is quite easily differ from *S. eurynotus* by its subequal width and length, shallower ambulacrum III, more strongly wedge-shaped profile, small size, non-angular posterior part and apex is less eccentric than *S. eurynotus.* Anterior ambulacrum (III) is deeply sunken in *S. eurynotus*, it is less steep in *S. parkinsoni*. In *S. parkinsoni* the rear ambulacral area is smaller while the interambulacral area is larger than *S. eurynotus.* Additionally, the shape of the peripetalous and lateral fascioles are the other criteria for distinguishing the specious. Furthermore,

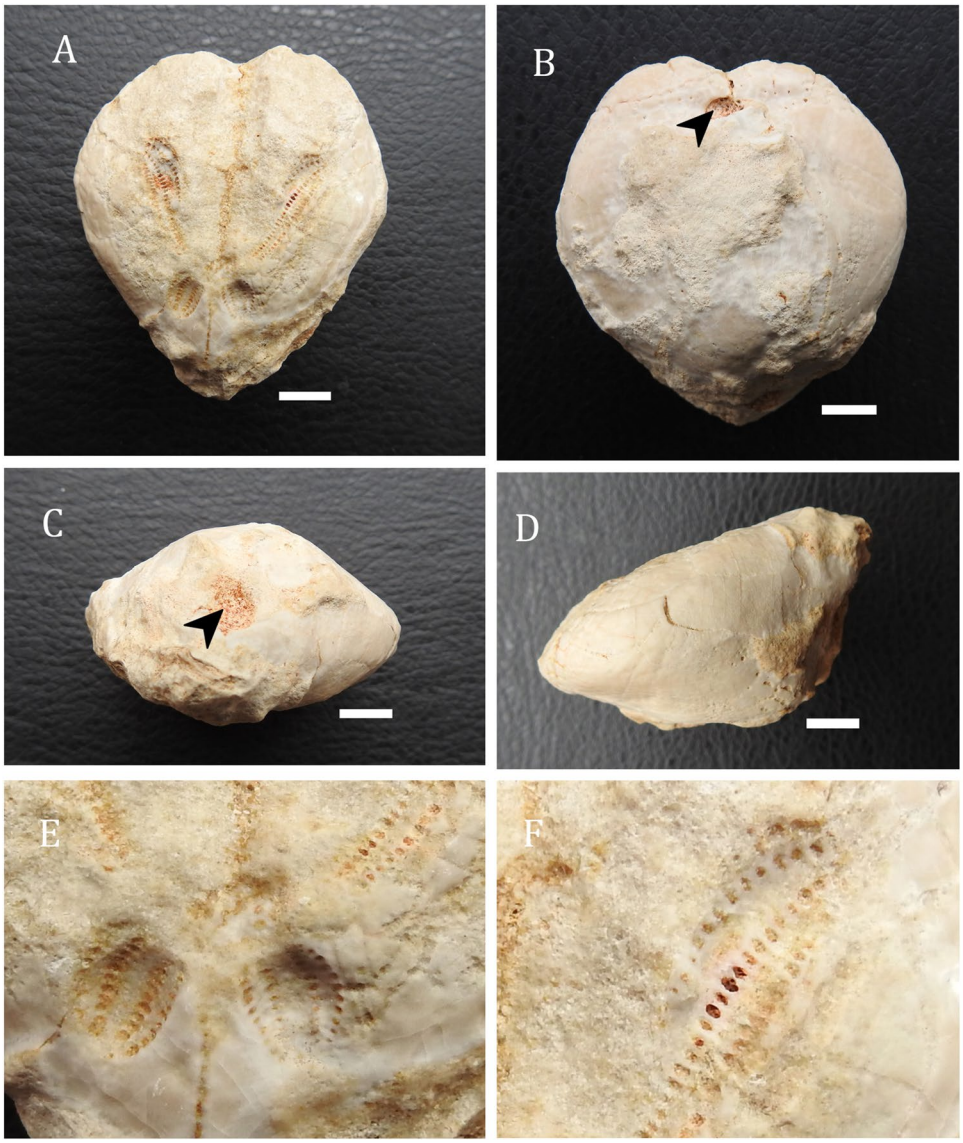

Fig. 12 *Schizaster parkinsoni* (Defrance 1827) (specimen SCP-1). **A** Apical view, **B** ventral view (arrow shown peristome), **C** posterior view (view of the periproctal area showed with arrow), **D** lateral view and **E** close-up posterior petaloid pairs. **F** close-up ambulacrum II with pairs of porus, each white scale bar equals 10 mm

S. parkinsoni is an intermediate form between *S. scillae* and *S. eurynotus* and has two gonopores in the apical system.

***Schizaster parkinsoni* Defrance, 1827 (specimen *SCP-1*) (Fig. 12)** Figure 12 L: 55 mm, W: 52 mm, H: 28 mm

Description: The test is heart-shaped, in subequal length and width. It has a wedge-shaped profile (Fig. 12D). Although ambulacra III is not fully seen, its length and depth can be distinguished (Fig. 12A). The peristome is seen on the ventral surface and close to the axes of the anterior ambulacrum III (Fig. 12B). The pericropt is located on the back pointed tip, located on moderately protruded posterior truncation, which can be visible from below (Fig. 12C). The apical system is at the posterior of the test at a ratio of 3 to 1. The distal part of the anterior petaloid tends to slightly outward (Fig. 12F). The posterior petaloid pair is almost one-fourth of the anterior petaloid pair (Fig. 12E). Pore pairs of the ambulacra II (Fig. 12F) and IV can be visible.

***Schizaster parkinsoni* Defrance 1827, (specimen *SCP-2*) (Fig. 13)** Figure 13 L: 53 mm, W: 49 mm, H: 28 mm

Description: The test is heart-shaped, in subequal length and width (Fig. 13A). It has a wedge-shaped profile (Fig. 13C). The apical system is in the posterior part (ratio of 3 to 1). The anterior petaloid pair tends slightly outward laterally (Fig. 13A). Pericropt and peristome do not appear due to poor preservation. One of the posterior petals is not visible, and the other is partially visible. The posterior part is outward. Since the anterior petaloid is filled with soil, its depth is not exactly understood. Spine tubercles are seen on some parts of the test (Fig. 13F). The posterior side formed a pointed protrusion.

Schizaster lovisatoi Cotteau 1895 (Fig. 14)

1895 *Schizaster lovisatoi*, Cotteau, p. 45, pl. 5, fig. 9, 10.
1907 *Schizaster calceolus*, Lambert, p. 69, pl. 5, fig. 8.

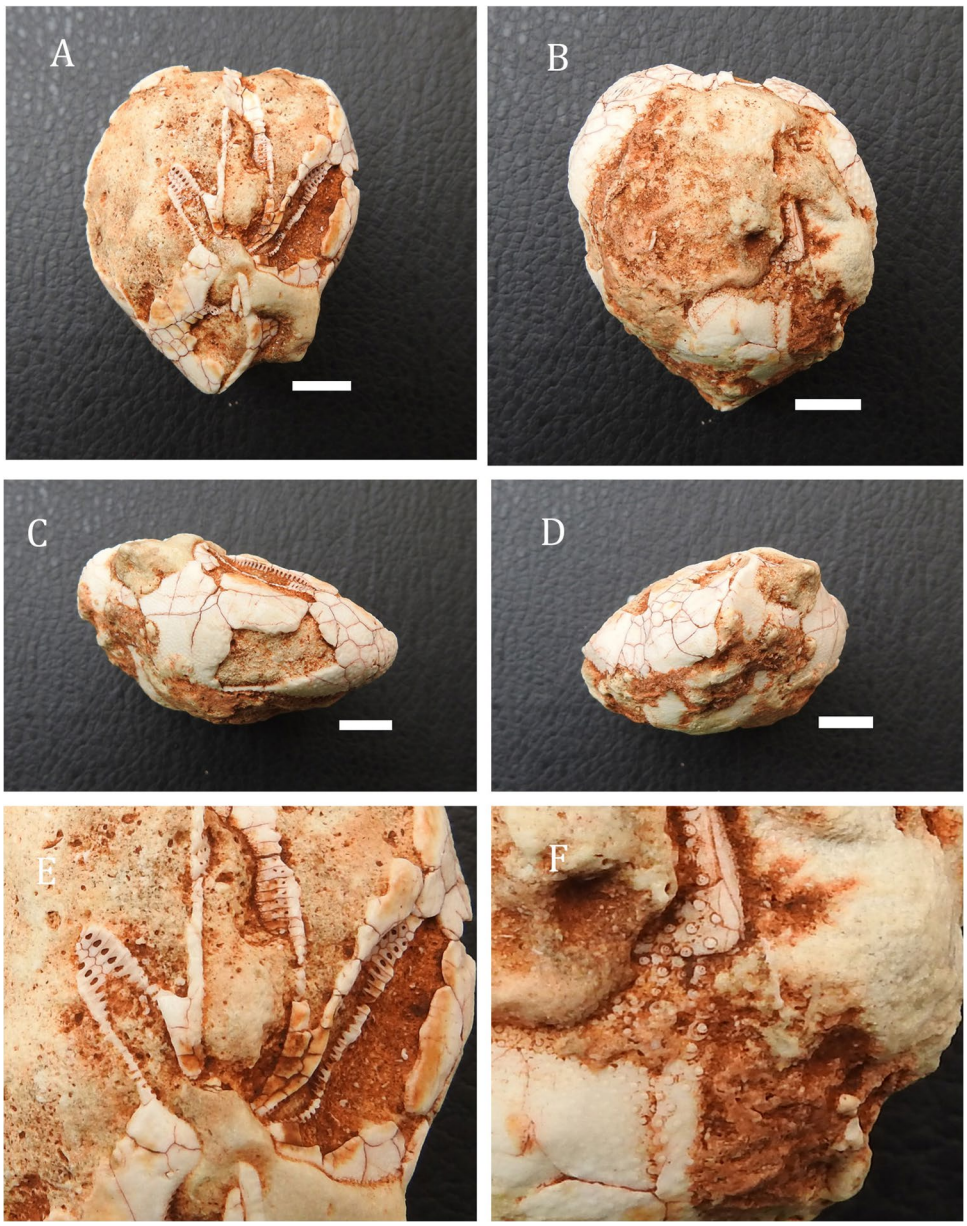

Fig. 13 *Schizaster parkinsoni* (Defrance 1827) (specimen *SCP-2*). **A** Apical view, **B** ventral view, **C** lateral view, **D** posterior view and **E** close-up of ambulacrum III, II and IV and apical disc, pair of pores in ambulacrum II and IV. **F** Close-up of the ventral surface and spine tubercles. Each white scale bar equals 10 mm

1913 *Schizaster lovisatoi*, Cottreau, p. 118, fig. 32, pl. 13, figs. 2, 7.

2017 *Schizaster lovisatoi*, Abdelhamied Elattaar, p. 250, pl. 7(3, 3a, 3b, 3c, 5).

Diagnostic features and remarks

Test is high and suboval with a moderately deep anterior sulcus. Anterior petals are longer than the posterior petals. Apex is slightly posterior, at the apical system. Apical disc has two gonopores. The peristome is kidney-shaped. Periproct is on the posterior part of truncation and nearly ovate. Pore-pairs are in single-column series, specialized for funnel-building tube-feet. *S. lovisatoi* differs from *S. eurynotus*, in having a higher test, wider posterior end, less oblique backward posterior truncation, smaller periproct and different shape of peripetalous fasciole on interambulacral II and IV. *S. lovisatoi* differs from *S. legraini* in having deeper and narrower frontal sinus, smaller periproct, a greater number of pore pairs in posterior petals relative to anterior ones and more oblique backward posterior truncation.

***Schizaster lovisatoi* Cotteau 1895, (specimen SCL) (Fig. 14)** Figure 14 L: 59 mm, W: 55 mm, H: 30 mm

Description: Test is high and suboval. The outer surface of the test is well preserved. Apex is slightly posterior, at the apical system (Fig. 14A). The apical disc is located close to 3/5 of its length. Ambulacrum III is in a deep groove from the apical centre to peristome part; however, in SCL, it is not exactly visible due to petrified soil. Pair of pores is not seen in any of the petaloid due to soil fragments. Anterior paired petals (II, IV) are longer than the posterior petaloid pair, a width of about one-third the length.

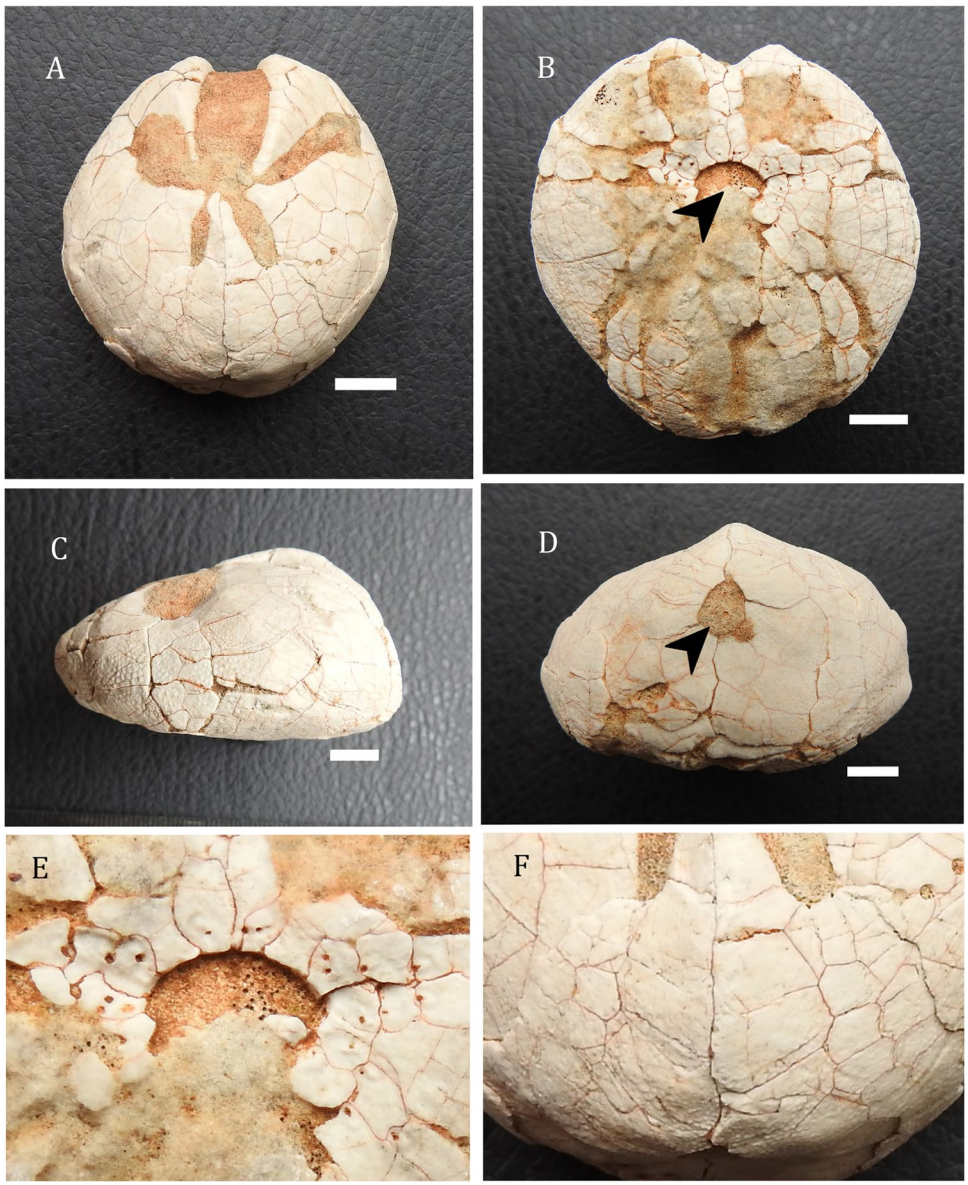

Fig. 14 *Schizaster lovisatoi* (Cotteau 1895) (specimen SCL). **A** Apical (aboral) view, **B** ventral (oral) view (arrow shows the peristome), **C** lateral view, **D** posterior view (view of the periproctal area) and **E** close-up peristome. **F** Detail of ventral surface of posterior. Each white scale bar equals 10 mm

The peristome is kidney-shaped (Fig. 14B, E) and close to the anterior part, a width of about one-fourth the length (Fig. 14B). Periproct is on the posterior part of truncation and can be visible from below. It is on the high side of the posterior, nearly ovate (Fig 14D). There is an upward projection on the posterior side.

Discussion

The description of the fossil or extant echinoids, particularly the clypeasteroids and spatangoids, often includes an explanation concerning the shape of the test, but this feature should never be used alone to indicate a species because it can vary even within a species. *Clypeaster* is irregular echinoids including the sand dollars and sea biscuits which are known as common shallow-water echinoids in tropical and subtropical seas and live in soft sediments from the littoral zone down to nearly 500 m (Kroh and Smith 2010; Mihaljević et al. 2011; Mihaljević and Rosenblatt 2018; Rahiminejad et al. 2020). They are deposited-feeders that have evolved with their large specific structural morphology and have a sophisticated feeding strategy (Smith 1984; Barras 2008; Mancosu and Nebelsick 2016). Their most striking feature is having five respiratory petals extending from a central or non-central apical disc. Small pores named tube feet are numerous and occur throughout the test. Tube-feet is available over large areas on either side of the ambulacra, particularly for pulling and holding sand over the test. The periproct (anus) is situated on the oral (ventral) surface mostly in the posterior interambulacrum, either near the margin or near the peristome (mouth). In most of the samples, the peristome is on the central part of

the apical disc (on the ventral surface) and Aristotle's lantern exists. Most species possess ciliated food grooves on the ventral surface; in a few species, the food grooves reach the aboral (apical) surface. An excessive amount of small miliary spines are present on the test surface. The amount of large spines is relatively few and some species have several types of pedicellaria (Serafy and Fell 1985; Mihaljevic et al. 2011; Mancosu and Nebelsick 2016; Mihaljević and Rosenblatt 2018; Taku et al. 2019). Due to their very robust test structure, they have survived to the present day as one of the most common fossil samples in Tertiary.

Clypeaster is accepted to be very difficult to subdivide taxonomically because the test patterns of various species show an extensive gradation and difference. Gradation of features can be observed in test size and profile, media outline, tuberculation, ambulacra shape, and position of peristome and periproct (Mihaljević et al. 2011). A difficult situation, which undoubtedly caused the number of nominal species to rise suddenly, has been worsened by palaeontologists who have created new fossil species based on minor shape differences in the poorly preserved examples and without reference to the taxa described in other regions (Mihaljevic et al. 2011; Mihaljević and Rosenblatt 2018).

Spatangoids are microphagous feeders, previously considered as non-selective deposit feeders. Their peristome is located close to the anterior and, unlike clypeasteroids, they do not have Aristotle's lantern. The first plate of the posterior interambulacrum forms a liplike structure, the labrum that extends forward under the peristoma. The plastron that includes two enlarged, interambulacral plates is on the posterior of the labrum. The periproct is positioned posteriorly. Petals are available but not all are of uniform size or developed. Regardless of the condition of the petals, they are generally bilaterally symmetrical. The tube feet are modified for some significant purposes such as respiration in petals, tunnel building, feeding around the mouth and maintenance in the anterior ambulacrum and around the periproct. The apical disc can be positioned centrally, anteriorly or posteriorly (Serafy and Fell 1985; Smith and Stockley 2005; Ghasemi Pour Afshar et al. 2015; Mooi 2020). Compared to the rapidly disintegrating ophiuroid, crinoid and asteroid skeletons, clypeasteroid and spatangoid tests can usually be maintained for millions of years after death due to their robust test structures and habit of embedding into the sand (Stockley et al. 2005; Mooi 2020). For example, *S. parkinsoni* (Figs. 12 and 13) and *S. eurynotus* (Figs. 10 and 11) are interpreted to have lived burrowing in fine-grained sands mostly because of their wedge-shaped profile. In addition, in comparison with *S. parkinsoni* and *S. eurynotus* possessing a deeper frontal ambulacrum, posteriorly located apical system, longer and more curve anterior-paired petaloid and shorter posterior-paired petaloid, is interpreted to have burrowed deeper in fine-grained sediments than *S. parkinsoni* (Mancosu and Nebelsick 2016). Because of these features, it has been possible that the tests of the fossil specimens have conserved to the present day without much deterioration.

Clypeasteroids fossils are prevalent and characteristic of many Cenozoic shallow-water deposits, particularly in the Mediterranean region, leaving numerous fossil records, like *Clypeaster*, *Parascutella*, *Echinocyamus*, *Scutella* and *Amphiope* and carbonate and siliciclastic deposits from shallow to deeper shelf settings are the main strata for clypeasteroids (Nebelsick and Kroh 2002; Kroh and Nebelsick 2003; Tsaparas et al. 2007; Belaústegui et al. 2012, 2013; Mancosu and Nebelsick 2013, 2015, 2017a). Eastern Mediterranean, Anatolia, has a rich source of echinoid fossil records, particularly clypeasteroid and spatangoid species; however, they are still not sufficiently studied. In an old study on the description and stratigraphic range of echinoid species from the Ermenek area (Konya-central Anatolia), the existence of *S. eurynotus*, *Echinolampas doma*, *C. crassus* and *C. scillae* was mentioned (Sezginman 1978). Besides, Roman (1960) reported that Helvinen echinoids of Karaman region (Central Anatolia) are as follows: *C. pentadactylus*, *C. altus*, *C. scillae*, *C. pomai*, *C. partschi*, *C.* aff. *zanoni*, *C. crassus*, *C.* cf. *crassus*, *C. crassicostatus*, *C.* aff. *altus*, *C. alticostatus*, *C. tauricus*, *C. campanulatus*, *C. manini*, *C. zumoffeni*, *C. torquati*, *C. delgadoi*, *C. doma*, *C. modenai*, *C. angustatus*, *C.* aff. *olisiponensis*, *C. ventiensis* and *S. dilatatus*. As it turns out, these two studies (Roman 1960 and Sezginman 1978) are very old and the accuracy of the species has not been investigated so far. In addition, the photographs of the mentioned species were not used in the studies and were not discussed in detail. In the current study, 11 specimens are highlighted as *C. latirostris* (Michelin, 1861) (specimen CLL-1, CLL-2), *C. michelotti* (Agassiz, 1840) (specimen CLM), *C. altus* (Klein, 1734) (specimen CLA), *C. intermedius* (Des Moulins, 1837) (specimen CLI-1, CLI-2) and *S. eurynotus* (Sismonda, 1841) (specimen SCE-1, SCE-2), *S. parkinsoni* (Defrance, 1827), (specimen SCP-1, SCP-2) and *S. lovisatoi* (Cotteau 1895) (specimen SCL). Among them, only *C. altus* and *S. eurynotus* were mentioned in Roman (1960) and Sezginman (1978) studies from Central Anatolia. No study was found on the other species mentioned in the present study. The first time, these aforementioned species will be introduced to the scientific community for southeastern Anatolia. On the other hand, fossil records of clypeasteroids and spatangoids were reported in many Mediterranean-based studies. For example, in a study on the sedimentary succession of Borutta Formation of Porto Torres from early-middle Miocene of Northern Sardinia, it is stated that deposit-feeding irregular forms with a dominance of the spatangoids *Ova* and *Brissopsis* and the minute clypeasteroid *Echinocyamus*, and the spatangoids *Opissaster*, *Holanthus*, *Metalia* and *Hemipatagus* as well as *C. marginatus* are reported (Mancosu and Nebelsick 2017b). On the other hand, in a study based on echinoid records of

lower Miocene from Funtanazza, middle of Western Sardinia, 18 genera of regular and irregular echinoids are reported as specified by clypeasteroids (*Clypeaster*, *Echinocyamus*), camarodonts (*Genocidaris*, *Psammechinus*), cidaroids (*Prionocidaris*, *Tylocidaris*), spatangoid (*Spatangus*) and echinolampadoids (*Hypsoclypus*, *Echinolampas*). In the same study, it was emphasized that in the inner sublittoral environments, there was a higher variety of regular echinoids such as *Genocidaris*, *Prionocidaris*, *Tripneustes*, *Tylocidaris*, and irregular echinoids, such as *Clypeaster*, *Schizaster*, *Trachypatagus*, *Spatangus*, *Echinolampas*, *Echinocyamus*, *Hypsoclypus* and *Lovenia.* In external sublittoral environments, species such as spatangoid echinoids and *Stylocidaris* have been reported to be dominant. In the study, it was emphasized that the echinoid assemblages of Funtanazza are common in the Miocene sedimentary sequences in the Mediterranean region. Also in the study, it was stated that the only *Clypeaster* specimen identified at the species level with the complete test is *C. latirostris*. Other studied *Clypeaster* samples were fragmented or not well preserved (Mancosu and Nebelsick 2016). In the present study, the same species *C. latirostris* was identified with two *specimens coded as CLL-1 and CLL-2* (Figs. 4 and 5); relatively they are well preserved and at full test architectures. In line with the data obtained with this study and earlier, it can be concluded that *C. latirostris* had lived in shallow waters around the Mediterranean for years.

In a study by Tsaparas et al. (2007), they stated that the Tortonian sediments of Gavdos Island (Greece) from the Miocene have rich and diverse echinoid fauna. Clypeasteroid echinoids have been described as significant species of this fauna and are recognized as 16 taxa. Eleven of these are reported as new records for Gavdos Island. They emphasized that although the conservation status of some fossil specimens is not well preserved, the following species have been identified: *C. campanulatus*, *C. intermedius*, *C. altus*, *C. lamberti*, *C. crassus*, *C. cf. ventiensis*, *C. cf. di-Stefanoi*, *C. calabrus*, *C. tauricus*, *C. intermedius* (form *crassicostatus*), *C. portentosus.* Among the species, *C. campanulatus*, *C. calabrus*, *C. altus*, *C. cf. ventiensis* and *C. lamberti* are the species seen in Miocene Formations of the Mediterranean. Besides, the stratigraphic and geographical distributions of the *Clypeaster* species distributed in the Mediterranean in different epochs were also shown in detail in Tsaparas et al, (2007) study. As follows, *C. altus* (Klein, 1734) is as Burdigalian-early Miocene (Italy, Malta, Algeria); middle Miocene (Turkey, Greece, Sardinia, Algeria, Sicily, Malta, France); Tortonian (Greece, Hungary); middle Tortonian (Gavdos); Miocene (Greece, Algeria, Sicily, Malta, Turkey, Sardinia, France); Tortonian (Hungary, Greece). *C. calabrus* (Seguenza, 1880) is as middle-late Miocene (Greece); Aquitanian (Italy); Middle Miocene (Sicily, Italy); middle Tortonian (Gavdos). *C. campanulatus* (Schlotheim, 1820) is as middle Tortonian (Gavdos); middle Miocene (Turkey, Austria, Spain, France, Corsica, Sardinia, Valearides, Greece); Tortonian (Syria, Hungary, Greece, Cilice). *C. crassus* (Agassiz, 1861) is as early Miocene (France, Egypt, Sardinia, Corsica, Algeria); middle Tortonian (Gavdos); middle Miocene (Turkey, France); Tortonian (Hungary). *C.* cf *di-Stefanoi* (Checchia—Rispoli, 1916) is as middle Tortonian (Gavdos); Pliocene (Greece, Italy). *C. intermedius* (Des Moulins, 1837) is as early-late Neogene (Middle East, France, Corsica, Spain, Valearides, Algeria, Egypt, Italy); middle-late Miocene (Greece); middle Tortonian (Gavdos). *C. intermedius* (form *crassicostatus*) (Des Moulins, 1837) is as middle Tortonian (Gavdos); middle-late Miocene (North Africa, Europe, Middle East). *C. lamberti* (Lovisato, 1905) is as Miocene (Sardinia); early-middle Miocene (Hungary, Turkey, Sardinia); middle Tortonian (Gavdos); Middle-Late Miocene (Greece). *C. portentosus* (Des Moulins, 1837) is as middle Neogene (France, Corsica, Balearics, Kalavria, Hungary, Malta, South Algeria, Cyprus); Miocene (Italy); Middle Tortonian (Gavdos). *C. tauricus* (Desor, 1859) is as middle Tortonian (Gavdos); middle Neogene (Portugal); middle Miocene (Crete, Sardinia, Spain, Corsica, Malta, Syria); middle Tortonian (Gavdos). *C.* cf. *ventiensis* (Tournouer, 1878) is as Miocene (Katalonia, Sardinia); middle Tortonian (Gavdos). As is known, in the study of Tsaparas et al. (2007), there is data on the presence of *C. altus* in Turkey, but no data on *C. latirostris*, *C. michelotti* and *C. intermedius* were reported. Besides, the existence of *C. intermedius*, and some of the other *Clypeaster* species such as *C. scillae*, *C. calabrus* and *C. marginatus* which are found in the Mores Formation (Early Miocene) of Porto Torres Basin (northern Sardinia) were mentioned by Mancosu and Nebelsick (2017a). Also, the presence of *C. scillae* was reported in Slovenia locality which is very rarely detected in that locality (Lower and Middle Miocene) (Mikuž, 1998). Remarkably, the species identified and announced by the current study will make significant contributions to the previously formed *Clypeaster* library and the distribution of *C. latirostris*, *C. michelotti* and *C. intermedius* can be revised. In another paper, Clypeasteroids and Spatangoids taxa of the Miocene of lower Tagus and Algarve Basin (Portuguese) are reported as 11 Clypeasteroids such as *C. altus*, *C. marginatus*, *C. campanulatus*, *C. latirostris*, *C. olisiponensis*, *Amphiope bioculata*, *Echinocyamus* sp. (2 specimens), *Parascutella lusitanica*, *P. smithiana*, *Parmulechinus* sp. and 16 Spatangoids such as *Schizaster* sp., *S. eurynotus*, *Spatangus delphinus*, *Brissopsis crescentica*, *B. ottnangensis*, *Brissidae* sp., *Schizobrissus* sp., *Hemipatagus ocellatus*, *Echinocardium olisiponensis*, *Lovenia* sp., *Pericosmus* sp., *P. latus*, *Opissaster cotteri*, *Agassizia algarbiensis*, *Ova karreri* and *A. zitteli* (Pereira 2010). Likewise, in the present paper, *C. altus* (Fig. 7), *C. latirostris* (Figs. 4 and 5) and *S. eurynotus* (Figs. 10 and 11) fossils records were found for early Miocene of Southeastern Anatolia. The existence of *C. altus*, *C. latirostris* and *S. eurynotus* in the early Miocene, abided with the current study; however, other than that, the

faunal information about the *C. michelotti*, *C. intermedius*, *S. parkinsoni* and *S. lovisatoi* species has not been mentioned in the study of Pereira (2010). This suggests that Anatolia could be a different fauna, especially for *C. michelotti*, *S. parkinsoni* and *S. lovisatoi* which are not mentioned much more for Mediterranean Miocene Formations in the previous studies.

Conclusion

In summary, the data presented herein will add information to the *Clypeaster* and *Schizaster* fauna from early Miocene (Aquitanian–Burdigalian) of Fırat Formation and the palaeogeographic distribution of the species from Diyarbakır (Eğil), the Southeastern Anatolia. *C. latirostris* (Michelin, 1861*)*, *C. michelotti* (Agassiz, 1840*)*, *C. altus (Klein*, *1734) C. intermedius* (Des Moulins, 1837), *S. eurynotus* (Sismonda, 1841), *S. parkinsoni* (Defrance, 1827) and *S. lovisatoi* (Cotteau 1895) species identified in the present study are considerable because of indicating the tropical climate of the region during early Miocene. The fossil species discussed here seem to prefer neritic and sandy-clay (limestone) habitats. These data will contribute to providing data for new paleoenvironmental studies by palaeontologists and geologists, and be a pioneer for new fossil records and palaeological studies. By the way, due to Turkey's geological formation, echinoid fossils deposition of Anatolia is quite abundant; however, considering the lack of palaeontological investigations, we still believe that no significant amount of studies has been conducted.

Acknowledgements I want to offer my most sincere thanks to Dr Nikolaos Tsaparas and Dr Nurdan İnan who have contributed to the identification of the genus and species. The author also thanked İrfan Buğday and Müjdat Kılıç for technical support of the computer programme. Furthermore, the author would like to thank the students of Diyarbakir/Eğil-Sağlam Secondary School and their principal Bekir Ekin and teacher Arzu Ekin who contributed to the collection of the fossils and determining their areas.

Author contribution IE designed and wrote the article, surveyed the field works, analysed the data and organized them in figures.

Declarations

Conflict of interest The author declares no competing interests.

References

Alvarado, J.J., Cortés, J. 2009. Echinoderms. In: Wehrtmann, I.S., Cortés, J. (eds) Marine Biodiversity of Costa Rica, Central America. Monographiae Biologicae, vol 86. Springer, Dordrecht. https://doi.org/10.1007/978-1-4020-8278-8_39

Barras CG (2008) Morphological innovation associated with the expansion of atelostomate irregular echinoids into fine-grained sediments during the Jurassic. Palaeogeogr Palaeoclimatol Palaeoecol 263(1–3):44–77. https://doi.org/10.1016/j.palaeo.2008.01.026

Belaústegui Z, De Gibert JM, Nebelsick JH, Domènech R, Martinell J (2013) Clypeasteroid tests as a benthic island for gastrochaenid bivalve colonization: evidence from the Middle Miocene of Tarragona, North-East Spain. Palaeontology 56:783–796. https://doi.org/10.1111/pala.12015

Belaústegui Z, Nebelsick JH, De Gibert JM, Domènech R, Martinell J (2012) A taphonomic approach to the genetic interpretation of clypeasteroid accumulations from Tarragona (Miocene, NE Spain). Lethaia 45:548–565. https://doi.org/10.1111/j.1502-3931.2012.00314.x

Cotteau G (1895) Description des échinides recueillis par M. Lovisato dans le Miocène de la Sardaigne. Mémoires De La Société Géologique De France, Paléontologie 13:5–56

Dickson JAD (2004) Echinoderm skeletal preservation: Calcite-Aragonite Seas and the Mg/Ca ratio of Phanerozoic Oceans. J Sediment Res 74(3):355. https://doi.org/10.1306/112203740355

Duke WL, Arnott RWC, Cheel RJ (1991) Shelf sandstones and hummocky cross-stratification: New insights on a stormy debate. Geology 19(6):625–628. https://doi.org/10.1130/0091-7613(1991)019%3c0625:SSAHCS%3e2.3.CO;2

Flower BP, Kennett JP (1994) The middle Miocene climate transition, East Antarctic ice sheet development, deep ocean circulation and global carbon cycle. Palaeogeography, Paleoclimatology, Paleoecology 108(3–4):537–555. https://doi.org/10.1016/0031-0182(94)90251-8

Genç S (1985) Bitlis Masifi Lice-Kulp (Diyarbakır) ve Çökekyazı-Gökay (Hizan, Bitlis) yöreleri gnays ve amfibolitlerinin köken sorununun irdelenmesi. (Discussion on the parent problem of gneisses und amphibolites in the Lice-Kulp (Diyarbakır) and Çökekyazı-Gökay areas of the Bitlis masif). Jeoloji Mühendisliği 23:31–38 (**(in Turkish)**)

Ghasemi, Pour, Afshar, Y., Vaziri, M., Dastanpour, M., Lotfabad, Arab, A. 2015. Lutetian Schizaster Fauna (Echinoidea, Spatangoida) from Sargaz Area, South of Kerman, Iran. Journal of Sciences, Islamic Republic of Iran, 26(2), 131–138. https://www.sid.ir/en/journal/ViewPaper.aspx?id=661496

Ghiold J, Hoffman A (1986) Biogeography and biogeographic history of clypeasteroid echinoids. J Biogeogr 13(3):183–206. https://doi.org/10.2307/2844920

Güngör Yeşilova P, Helvacı C (2017) Petrographic study and geochemical investigation of the evaporites associated with the Germik Formation (Siirt Basin, Turkey). Carbonates Evaporites 32:177–194. https://doi.org/10.1007/s13146-015-0285-y

Güngör Yeşilova, P., Helvacı, C. 2013. Kurtalan sahası (GB Siirt) Germik formasyonu oligosen evaporitlerinin diyajenezi ve paleocoğrafik gelişimi, Türkiye. (Diagenesis and Paleogeographic Development of Oligocene Evaporites of the Germik Formation (Kurtalan, SW Siirt), Turkey). Yerbilimleri Dergisi, 34(1), 1–22. (in Turkish). https://dergipark.org.tr/en/pub/yerbilimleri/issue/13651/165227

Greenop R, Foster GL, Wilson PA, Lear CH (2014) Middle Miocene climate instability associated with high amplitude CO_2 variability. Paleoceanography 29. https://doi.org/10.1002/2014PA002653

Greenstein BJ (1995) The effects of life habit and test microstructure on the preservation potential of echinoids in Graham's Harbour, San Salvador Island, Bahamas. Geol Soc Am Spec Pap 300:177–188. https://doi.org/10.1130/0-8137-2300-0.177

Hüsing SK, Zachariasse WJ, Van Hinsbergen DJJ, Krijgsman W, Inceöz M, Harzhauser M, Mandic O, Kroh A (2009) Oligocene-Miocene basin evolution in SE Anatolia, Turkey: constraints on the closure of the eastern Tethys gateway. Geological Society London Special Publications 311(1):107–132. https://doi.org/10.1144/SP311.4

İnan, N. 2008. Türkiyenin önemli omurgasız fosilleri (Important Invertebrate Fossils of Turkey), TUBITAK, Popular Science Books, No: 287, p 138, TUBITAK, Ankara.

Kathleen N (2010) Landscape development within a young collision zone: implications for post-Tethyan evolution of the Upper Tigris River system in Southeastern Turkey. Int Geol Rev 52(4):404–422. https://doi.org/10.1080/00206810902951072

Keskin M (2003) Magma generation by slab steepening and breakoff beneath a subduction accretion complex: An alternative model for collision-related volcanism in Eastern Anatolia. Turkey Geophysical Research Letters 30(24):8046–8050. https://doi.org/10.1029/2003GL018019

Kroh A, Nebelsick JH (2003) Echinoid assemblages as a tool for palaeoenvironmental reconstruction-An example from the Early Miocene of Egypt. Palaeogeogr Palaeoclimatol Palaeoecol 201:157–177. https://doi.org/10.1016/S0031-0182(03)00610-2

Kroh A, Smith AB (2010) The phylogeny and classification of post-Palaeozoic echinoids. J Syst Paleontol 8(2):147–212. https://doi.org/10.1080/14772011003603556

Lambert J (1906) Etude sur les Echinides de la molasse de Vence. Annales De La Société Des Lettres, Sciences Et Arts, Alpes-Maritimes, Nice 20:1–64

Mancosu A, Nebelsick JH (2017a) Palaeoecology and taphonomy of spatangoid-dominated echinoid assemblages: A case study from the Early-Middle Miocene of Sardinia, Italy. Palaeogeogr Palaeoclimatol Palaeoecol 466:334–352. https://doi.org/10.1016/j.palaeo.2016.11.053

Mancosu A, Nebelsick JH (2013) Multiple routes to mass accumulations of clypeasteroid echinoids: A comparative analysis of Miocene echinoid beds of Sardinia. Palaeogeogr Palaeoclimatol Palaeoecol 374:173–186. https://doi.org/10.1016/j.palaeo.2013.01.015

Mancosu A, Nebelsick JH (2015) The origin and paleoecology of clypeasteroid assemblages from different shelf setting of the Miocene of Sardinia. Italy Palaios 30(5):273–387. https://doi.org/10.2110/palo.2014.087

Mancosu A, Nebelsick JH (2016) Echinoid assemblages from the early Miocene of Funtanazza (Sardinia): a tool for reconstructing depositional environments along a shelf gradient. Palaeogeogr Palaeoclimatol Palaeoecol 454:139–160. https://doi.org/10.1016/j.palaeo.2016.03.024

Mancosu A, Nebelsick JH (2017b) Ecomorphological and taphonomic gradient of clypeasteroid-dominated echinoid assemblages along a mixed siliciclastic-carbonate shelf from the early Miocene of northern Sardinia. Italy Acta Palaeontologica Polonica 62(3):627–648. https://doi.org/10.4202/app.00357.2017

Mihaljević, M., Jerjen, I., Smith, A.B. 2011. The test architecture of Clypeaster (Echinoidea, Clypeasteroida) and its phylogenetic significance. Zootaxa, 2983, 21–38. https://doi.org/10.11646/zootaxa.2983.1.2

Mihaljević M, Rosenblatt AJ (2018) A new fossil species of *Clypeaster* (Echinoidea) from Malaysian Borneo and an overview of the Central Indo-Pacific echinoid fossil record. Swiss Journal of Palaeontology 137:389–404. https://doi.org/10.1007/s13358-018-0164-y

Mikuž V (1998) *Clypeaster scillae* Des Moulins, 1837 from Miocene beds near Podgračeno, Eastern Slovenia. Geologija 41:109–116. https://doi.org/10.5474/geologija.1998.006

Mooi R (1989) Living and fossil genera of the Clypeasteroida (Echinoidea: Echinodermata): An illustrated key and annotated checklist. Smithsonian Contributions to Zoology 488:1–51. https://doi.org/10.5479/si.00810282.488

Mooi, R. 2020. Spatangoida. In: AccessScience. McGraw-Hill Education. https://doi.org/10.1036/1097-8542.640800

Nebelsick, J.H., Kroh, A. 2002. The stormy path from life to death assemblages: The formation and preservation of mass accumulation of fossil sand dollars. Palaios, 17(4), 378–393. https://www.jstor.org/stable/3515762

Pereira P (2010) Echinoids (Echinodermata) from the Neogene of Portugal mainland: systematics review. Publicaciones Del Seminário De Paleontologia De Zaragoza 9:205–208

Rahiminejad AH, Yazdi M, Bahrami A (2020) Palaeoenvironments and taphonomy of clypeasteroids in Miocene carbonates of the Esfahan-Sirjan Basin, central Iran. Facies 66:14. https://doi.org/10.1007/s10347-020-00598-6

Roman, J. 1960. Karaman havzası helvesien ekinidleri (Clypeaster, Scutella, Schizaster) Maden Tetkik Arama Enstitüsü Dergisi, 55, 52–82. (in Turkish). https://dergipark.org.tr/tr/download/article-file/626070

Şenel M (2002) Geological map of Turkey. General Directorate of Mineral Research and Exploration Publication, Ankara-Turkey, MTA

Şengör AMC, Yılmaz Y (1981) Tethyan evolution of Turkey: a plate tectonic approach. Tectonophysics 75:181–241

Serafy, D.K., Fell, F.J. 1985. Marine flora and fauna of the Northeastern United States. Echinodermata: Echinoidea. NOAA Technical Report National Marine Fisheries Service, 33, 1–27. http://spo.nwr.noaa.gov/tr33.pdf

Sezginman Y (1978) Ermenek (Konya) Bölgesinden toplanmış ekinit türlerinin tanımlamaları ve stratigrafik yayılımları (Description and stratigraphic range of echinid species collected from the Ermenek Area (Konya). Bulletin of the Geological Society of Turkey 81:43–50 ((**in Turkish**))

Smith AB (1984) Echinoid Palaeobiology. George Allen and Unwin Ltd., London

Smith AB (2001) Probing the cassiduloid origins of clypeasteroid echinoids using stratigraphically restricted parsimony analysis. Paleobiology 27(2):392–404. https://doi.org/10.1666/0094-8373(2001)027%3c0392:PTCOOC%3e2.0.CO;2

Smith AB, Stockley B (2005) Fasciole pathways in spatangoid echinoids: a new source of phylogenetically informative characters. Zool J Linn Soc 144(1):15–35. https://doi.org/10.1111/j.1096-3642.2005.00161.x

Stockley B, Smith AB, Littlewood T, Lessios HA, Mackenzie-Dodds JA (2005) Phylogenetic relationships of spatangoid sea urchins (Echinoidea): Taxon sampling density and congruence between morphological and molecular estimates. Zoolog Scr 34(5):447–468. https://doi.org/10.1111/j.1463-6409.2005.00201.x

Taku, H., Takuya, M., Atsuko, A. 2019. Chapter 4 - Cidaroids, clypeasteroids, and spatangoids: Procurement, culture, and basic methods. Methods in Cell Biology, 150, 81–103. https://doi.org/10.1016/bs.mcb.2018.09.012.

Tsaparas, N., Drinia, H., Antonarakou, A., Marcopoulou-Diakantoni, A., Dermitzakis, M.D. 2007. Tortonian *Clypeaster* fauna (Echinoidea: Clypeasteroida) from Gavdos Island (Greece). Bulletin of the Geological Society of Greece, 40, 225–237. https://doi.org/10.12681/bgsg.16531

Walker, D.E, Gagnon, J.M. 2014. Locomotion and functional spine morphology of the heart urchin *Brisaster fragilis*, with Comparisons to *B. latifrons*. Journal of Marine Sciences, ArticleID 297631, 9 pages. https://doi.org/10.1155/2014/297631

Woodruff F, Savin S (1991) Mid-Miocene isotope stratigraphy in the deep sea: High-resolution correlations, paleoclimatic cycles, and sediment preservation. Paleoceanography 6(6):755–806. https://doi.org/10.1029/91PA02561

Yeşilova Ç, Helvacı C, Carrillo E (2018) Evaporitic sedimentation in the Southeastern Anatolian Foreland Basin: New insights on the Neotethys closure. Sed Geol 369:13–27. https://doi.org/10.1016/j.sedgeo.2018.03.012

Yeşilova, Ç., Helvacı, C. 2012a. Batman-Siirt kuzeyi stratigrafisi ve sedimantolojisi, Türkiye. Türkiye Petrol Jeologları Dergisi, 23(2), 7–49. (in Turkish) http://www.tpjd.org.tr/images/bultenler/pdf/aralik2011.pdf

Yeşilova, Ç., Helvacı, C. 2012b. Lice Formasyonu evaporitleri ve killerinin ekonomik önemi: Baykan-Kurtalan-Şirvan Bölgesi (Siirt). Yüzüncü Yıl Üniversitesi Fen Bilimleri Dergisi, 17(2), 77–83. (in Turkish). https://dergipark.org.tr/tr/pub/yyufbed/issue/21967/235856

Yılmaz E, Duran O (1997) Güneydoğu Anadolu bölgesi otokton ve allokton birimler stratigrafi adlama sözlüğü (Lexicon). TPAO Araştırma Merkezi Grubu Başkanlığı Eğitim Yayınları 3:460 ((**in Turkish**))

Yılmaz Y (1993) New evidence and model on the evolution of the Southeast Anatolian orogen. Geological Society of American Bulletin 105(2):251–271. https://doi.org/10.1130/0016-7606(1993)105%3c0251:NEAMOT%3e2.3.CO;2

Zachos J, Pagani M, Sloan L, Thomas E, Billups K (2001) Trends, rhythms, and aberrations in global climate 65 Ma to present. Science 292(5517):686–693. https://doi.org/10.1126/science.1059412

Ziegler A, Gilligan AM, Dillon JG, Pernet B (2020) Schizasterid heart urchins host microorganisms in a digestive symbiosis of Mesozoic origin. Front Microbiol 11:1697. https://doi.org/10.3389/fmicb.2020.01697